1

METAL–POLYMER NANOCOMPOSITES BY SUPERCRITICAL FLUID PROCESSING

T. Hasell

Department of Chemistry, University of Liverpool, Liverpool, UK

1.1 INTRODUCTION TO POLYMERS, NANOPARTICLES, AND SUPERCRITICAL FLUIDS

Nanoparticles
A nanoparticle is defined by the British Standards Institution as follows:
Nanoparticle*—particle with one or more dimensions at the nanoscale*
Nanoscale*—having one or more dimensions of the order of 100 nm or less*
This is in good agreement with how the term is used in general within the scientific community, although there is some degree of ambiguity as to the upper size limit. Particles and materials with the smallest domain sizes up to a micrometer and even several micrometre are sometimes referred to as "nano," although this is becoming less common with the increasing standardization of terminology in nanoscience.

1.2 PROPERTIES

Over the last three decades, nanoparticles have received an increasing amount of research interest. This is due to the unique size-dependent properties of nanoparticles, which are often thought of as a separate and intermediate state of matter lying between

---

Nanocomposites: In Situ *Synthesis of Polymer-Embedded Nanostructures*, First Edition.
Edited by Luigi Nicolais and Gianfranco Carotenuto.

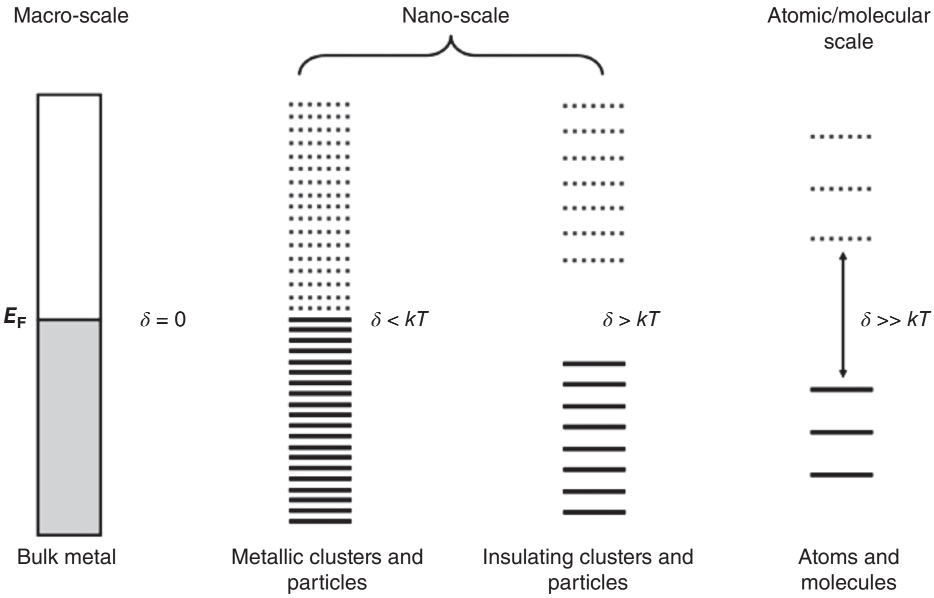

Figure 1.1. The evolution of the band gap and the density of states as the number of atoms in a system increases (from right to left). E_F is the Fermi energy level of the material and δ is the Kubo gap; see related text. Adapted from Roduner [2]. Reproduced by permission of The Royal Society of Chemistry.

individual atoms and bulk material. The properties of nanoparticles arise as a consequence of the confinement of the electron wave function and of the extremely high proportion of surface atoms—both of these factors are directly dependent on the size of the nanoparticle [1]. Indeed the possibility to control the properties, by tuning the size of the nanoparticle, has been the cause and subject of much investigation. Unlike bulk materials that have constant physical properties regardless of mass, nanoparticles offer unique opportunities for control by varying the diameter and have electronic, magnetic, and optical properties that can be manipulated. These effects occur because the energy levels for small particles are not continuous, as in bulk materials, but discrete, due to confinement of the electron wave function. The physical properties of nanoparticles are therefore determined by the size of the particle, the relatively small physical dimension in which the wave function is confined (Fig. 1.1).

The Fermi energy level (E_F) is the highest occupied energy level of the system in its ground state (lowest energy). The band gap (E_g) of these systems is the energy gap between the highest occupied and lowest unoccupied energy states. In these systems, from discrete atoms to bulk materials, the energy spacings are determined by the extent of the overlap between the electron orbitals of the material. Individual atoms have well-known atomic orbitals. These can combine in molecules to form molecular orbitals and further to form extended band structures, as in metals or semiconductors. The value of E_g is proportional to E_F divided by the number of delocalized electrons in the extended band structure. For a bulk metal, the number of delocalized electrons in the band structure is equal to the number of atoms in the bulk of the material. This normally results in E_g being very small and therefore only observable at low temperature. Under normal temperature, the delocalized electrons of the metal can be promoted easily to a higher energy state and can move freely through the structure. This gives the material its electrically conductive nature. In traditional semiconductor materials, the number of delocalized electrons is significantly less than the number of atoms. This results in a higher E_g that is significant at normal temperatures. This means that in a semiconductor the electrons will not be free to move, and conduct current, without some further input of energy. Equation 1.1 gives the average electronic energy level spacing of successive quantum levels (known as the Kubo gap):

$$\delta = \frac{4E_F}{3n} \tag{1.1}$$

where δ is the Kubo gap, E_F is the Fermi energy level of the bulk material, and n is the total number of valence electrons in the nanoparticle

As an example, a silver nanoparticle of 3 nm diameter and ~1000 atoms (and therefore ~1000 valence electrons) would have a δ value of about 5–10 meV [1]. If the thermal energy, kT, is more than the Kubo gap, then the nanoparticle would be metallic in nature, but if kT fell below the Kubo gap, it would become nonmetallic. At room temperature, kT is ~26 meV, and therefore a 3 nm silver nanoparticle would exhibit metallic properties. However, if the size of the nanoparticle was decreased or the temperature was lowered, the nanoparticle would show nonmetallic behavior. Using this theory and a Fermi energy for bulk silver of 5.5 eV, then silver nanoparticles should cease to be metallic when under ~280 atoms, at room temperature. Because of the Kubo gap in nanoparticles, properties such as electrical conductance and magnetic susceptibility exhibit quantum size effects. These effects have led to nanoparticles being used for many applications from catalysis to optics and medicine.

1.3 CATALYSIS

The efficiency of materials already used as catalysts would be expected to be higher for nanoparticles than other solid substrates even by conventional theory. This is simply because nanoparticles have a much larger proportion of atoms in active surface sites compared to larger objects (see Fig. 1.2). Nanoparticles are so close in size to atomic dimensions that an unusually high fraction of the atoms are present on the surface. It is possible to estimate this fraction by using the simple relation shown in Equation 1.2:

$$P_s = 4N^{-1/3} \times 100 \tag{1.2}$$

where P_s is the percentage of atoms at the surface of a metal particle and N gives the total number of atoms in the particle [3]

The 3 nm silver nanoparticle we used in the previous example would contain ~1000 atoms [1]. We can therefore estimate that it would have ~40% of the total number of

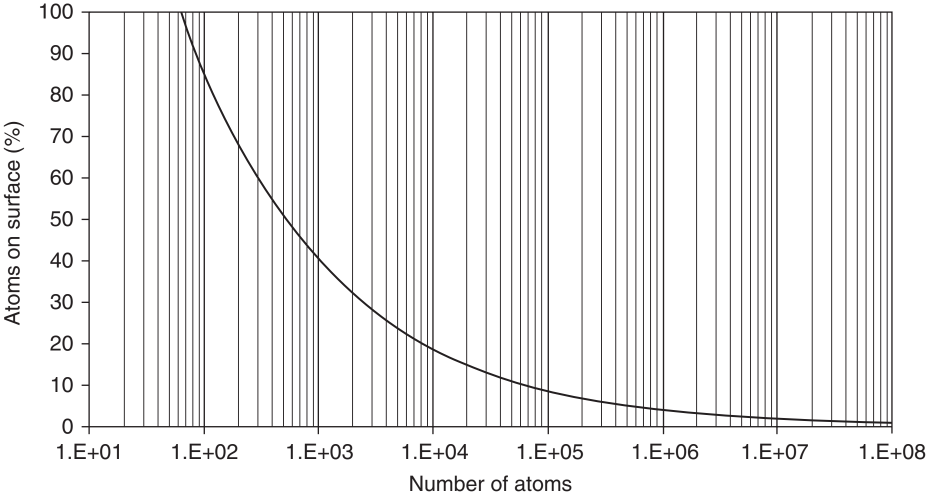

Figure 1.2. A plot of the total number of atoms in a metal particle vs. the percentage of those atoms that are located at the surface of the particle, derived from Equation 1.2.

atoms on the surface. A particle 150 nm in diameter would contain ~10^7 atoms, with less than 1% of the atoms in surface locations. As heterogeneous catalysis occurs only at the surface of the metal being used, it is obvious to see why the use of nanoparticles is advantageous in order to make optimum use of often expensive catalytic metals.

Aside from these simple surface/volume effects, there are changes in the reactivity of nanoparticles that arise from the quantum confinement effect. This qualitative change in the electronic structure can cause unusual catalytic properties in the nanoparticles that are quite different from the behavior of the bulk material. Photoemission spectroscopy investigations have shown that the electronic structure of metal clusters smaller than ~5 nm is different from that of the bulk metal [4]. The small number of atoms involved in the formation of the electron bands results in a greater localization of the valence electrons and in a smaller width of the valence band. This altered electronic structure and the force towards the center generated by the surface curvature of small metal nanoparticles give rise to a significant contraction of the lattice compared to the bulk material [5]. In turn, the smaller lattice constant is responsible for a shift of the center of the *d*-band to higher energies, which generally enhances the reactivity of the surface towards adsorbates.

There is also a dramatic increase in the number of edge and corner sites in the metal lattice—and these can react quite differently to the flat metal surface in terms of catalysis properties. The enhancement of the reactivity of low-coordination defect sites can be so large that their presence determines the catalytic activity of a material, in spite of their low concentration [4]. Gold provides an excellent example of a material that behaves markedly differently in the form of nanoparticles. Perhaps the largest breakthrough in nanoparticle catalysis was the work done by Haruta on gold nanoparticle-catalyzed CO oxidation by O_2 at low temperatures [6–8]. Gold is widely recognized as being chemically inert. It is indeed one of the most stable metals in the group 8 elements and is resistant to oxidation. The discovery that gold nanoparticles supported on Co_3O_4, Fe_2O_3, or TiO_2 were highly active catalysts for CO and H_2 oxidation, NO reduction, water-gas shift reaction, CO_2 hydrogenation, and catalytic combustion of methanol was therefore a surprise and considered important by the chemical community [9]. Smooth surfaces of metallic gold do not adsorb CO, and this is necessary for catalysis at room temperatures [10]. CO is instead only adsorbed at corner, step, and edge sites, indicating that smaller metallic gold nanoparticles are preferable [11].

Nanoparticles of a large range of transition metals and metal oxides have been found to exhibit advantageous size-dependent catalytic properties and are being investigated intensively. The shape, coordination, and stabilization of these nanoparticles have been found to affect the catalysis and are therefore also the subject of much current research. As with many other applications of nanoparticles, catalysis often requires a suitable support/substrate for the nanoparticles. This should ideally provide a convenient means to utilize the nanoparticles while protecting them from aggregation and allowing simple recovery. There is therefore much interest in finding effective methods of producing supported nanoparticle catalytic materials using substrates such as inorganic oxides, alumina, silica, and titania, as well as polymers.

1.4 OPTICS AND PHOTONICS

Nanomaterials interact with light differently from the bulk material. Materials in the micro-/nanosize range are of dimensions that are comparable to, or smaller than, the wavelength of light. If a material is of dimensions close to the wavelength of light and is surrounded by a substance of different refractive index, then light of appropriate wavelength will be scattered. The specific wavelength of light that is scattered is dependent on the thickness of the scattering phase. It is this effect that causes oil stretched thinly across the surface of water to produce rainbow colors. This effect has been used in optical materials known as photonic crystals, which are designed with phases of different refractive indices and specific dimensions and architectures intended to produce a desired interaction with light.

In the case of materials in which the separate phase is significantly smaller than the wavelength of light, this effect does not occur. Instead, the two phases behave as a single material with respect to the transmitted light. Therefore, transparent materials with embedded nanoparticles may still remain transparent to light even if the material the nanoparticles are formed from is opaque or reflective in its bulk form. Composites, transparent materials, and inorganic particles in the micrometer range, on the other hand, are often opaque. The light scattering, which is responsible for the opacity, is suppressed either by using materials with nearly matching refractive indices or by decreasing the dimensions of the filler to a range below c. 50 nm. Therefore, nanocomposites with embedded nanoparticles can act as homogeneous materials with modified properties. Instead of scattering light, a merging of the refractive indices of the nanoparticles and host material takes place. Nanoparticles with a high refractive index can be dispersed in a glass or polymer to increase the effective refractive index of the medium.

This approach is helpful in producing optical waveguides where a higher refractive index leads to better beam confinement [12].

Nanoparticles of conducting and semiconducting materials interact directly with light through different mechanisms. It is because of these properties that these nanoparticles are often added to an optical substrate to perform a desired function. Conducting metallic nanoparticles interact with light via an effect known as plasmon resonance, arising from the delocalized cloud of electrons associated with the particle. Semiconductor nanoparticles, often known as "quantum dots," interact with light according to exciton mechanisms modified by the quantum confinement effect. These will be dealt with separately. Quantum dots will only be described briefly as they are not directly relevant to the research reported later in this chapter but are included for comparison.

1.4.1 Quantum Dots

The most significant electronic effect in semiconductor nanoparticles is the widening of the gap between the highest occupied electronic states (at the top of the original valence band) and the lowest unoccupied states (the bottom of the original conduction band). This occurs through quantum confinement because of the small dimensions of the particle [13], which directly affects the optical properties of semiconductor nanoparticles as compared to the bulk material. The minimum energy needed to create an electron–hole pair in a semiconductor nanoparticle (an "exciton") is defined by its band gap (E_g). Light with energy lower than E_g cannot be absorbed by the nanoparticle; the onset of absorption is also size dependent. As the size decreases, the absorption spectra for smaller nanoparticles are shifted to shorter wavelengths; that is, the gap increases in size, with respect to larger nanoparticles or the bulk material.

Excitons in semiconductors have a finite lifetime because of recombination of the photoexcited electron–hole pair. In semiconductor nanoparticles, the energy released by this recombination is too large to be dissipated by vibrational modes. Instead, it is emitted in the form of a photon of appropriate energy. The energy for this fluorescence is centered at a value smaller than the energy required to generate the exciton. If narrow size distributions of quantum dots can be obtained, then a wide range of colors can be produced, even for the same semiconductor material, with each color associated with a different size.

1.4.2 Plasmons

Metallic nanoparticles can have absorption spectra with an absorption peak that looks similar to that of semiconductor nanoparticles. However, this absorption does not derive from transitions between quantized energy states; instead, in metal nanoparticles, collective modes of motion of the electron cloud can be excited [14]. Under the influence of an electrical field, there is a plasmon excitation of the electrons at the particle surface. This resonance takes place at a certain frequency of incident light and results in an optical absorption. These are referred to as surface plasmons, or also as plasma resonance absorption, or as localized surface plasmons.

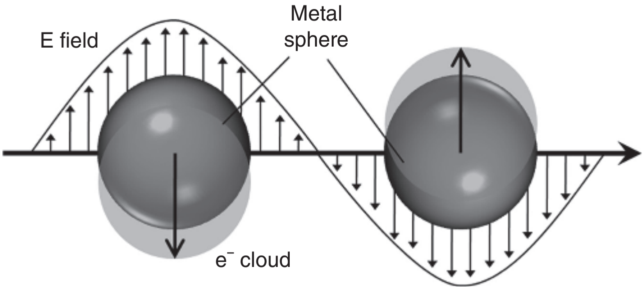

Figure 1.3. Schematic of plasmon oscillation for a sphere, showing the displacement of the conduction electron charge cloud relative to the nuclei, as described by Kelly et al. [17].

As particle size decreases, the conduction electrons begin to interact with the boundary of the particle [15]. A metal–dielectric boundary on the nanoscale produces considerable changes in the optical properties, making them size and shape dependent [16]. When a metallic nanoparticle is irradiated by light, the electric field of the incident light induces a coherent oscillation of the conduction electrons [17] (see Fig. 1.3). For nanoparticles significantly smaller than the wavelength of the light, absorption is within a narrow wavelength range, a plasmon band.

The width, position, and intensity of the plasmon interaction displayed by nanoparticles depend on [1, 16–19]:

- The dielectric functions of the metal and the host material
- Particle size and shape
- The interface between the particle and the host
- The distribution of particles within the host

Because of the influence of these factors, a desirable amount of control over the final properties of the material is possible, provided that an equal amount of control is possible in modifying the factors themselves. Different metals produce different light interactions and therefore colors. The extinction of light by metal nanoparticles occurs by both scattering and absorption mechanisms, but absorption is by far the dominant factor for nanoparticles of small size ($<20\,\text{nm}$). Nanosized metal particles have long been used for coloring glass from Roman times and through the Middle Ages in church windows. Although this particular application of nanoparticles may have been unintentional, small nanoparticles were often used to create glass with ruby-red Au and lemon-yellow Ag nanoparticles.

Today most of the use and study focuses on gold and silver nanoparticles because they exhibit the most pronounced plasmon effects and both have absorptions in the visible spectrum. Increasing the size of the particles, or increasing the dielectric constant of the medium, causes a redshift in the plasmon absorption [16]. However, it must be noted that the effect of nanoparticle size, though still significant, is considerably less dramatic than that observed in quantum dots. The absorption peak position in quantum dots is shifted markedly for a change in diameter of only fractions of a nanometer. For metal nanoparticles the shift in peak position is minimal for small particles (<25 nm for gold), although a broadening does take place. For larger metal particles (>25 nm for gold), the redshift of the plasmon resonance position is more significant [16]. If the particles are distorted in shape, then the plasmon band splits into different modes corresponding to the different aspects of the electron oscillations. For example, in a nanorod-shaped metallic nanoparticle, the plasmon band splits into two bands corresponding to oscillation of the free electrons along (longitudinal) and perpendicular (transverse) to the long axis of the rod. The transverse mode resonance is close to that observed for spherical particles, but the longitudinal mode is redshifted, dependent on the aspect ratio of the nanorod [16, 19].

Metal nanoparticles of this nature, intended for use in optical or photonic applications, are often embedded into a host material such as an appropriate polymer or glass. The incorporation of metal nanoparticles into optical substrates allows the construction of devices to utilize their advantageous properties. The host matrix not only forms the structure of the device but also protects the nanoparticles and prevents agglomeration. There are widespread uses for these emerging materials especially in optical and photonic applications including eye and sensor protection, optical communications, optical information processing, Raman enhancement materials, optical switching, plasmon waveguides, light-stable color filters, polarizers, and modified refractive index materials.

Silver nanoparticles are often singled out as an ideal choice of optically active nanoparticles for use in such research. Although silver and gold nanoparticles share many similar properties and applications, suitable silver feedstocks remain considerably more economically viable. In addition, silver represents the material with the most, and more general, applications. The reason for the considerable interest in the use of silver nanoparticles can best be summarized by reviewing the following statement from Reference [20]:

> Of the three metals (Ag, Au, Cu) that display plasmon resonances in the visible spectrum, Ag exhibits the highest efficiency of plasmon excitation. Moreover, optical excitation of plasmon resonances in nanosized Ag particles is the most efficient mechanism by which light interacts with matter. A single Ag nanoparticle interacts with light more efficiently than a particle of the same dimension composed of any known organic or inorganic chromophore. The light-interaction cross-section for Ag can be about ten times that of the geometric cross-section, which indicates that the particles capture much more light than is physically incident on them. Silver is also the only material whose plasmon resonance can be tuned to any wavelength in the visible spectrum. (Reference 20, 1222. Copyright Wiley-VCH Verlag GmbH & Co. KGaA. Reproduced with permission.)

From this statement the obvious advantages of silver, and the reason for its use as a model nanoparticle for the synthesis of nanocomposite materials, are clear. Noble metal nanoparticles have many applications; three major opportunities of these are outlined briefly in the succeeding text to demonstrate how these strong plasmon interactions can be utilized.

1.4.3 Nonlinear Optical Limitation

Many applications of optical composites of silver or gold nanoparticles derive from their potential as optical limiters. This arises from their nonlinear susceptibility near the surface plasmon frequency with picosecond response time [21]. Optical limitation is the decrease in absolute transmittance of a material as incident light fluence (energy per unit area) increases. Optical limiting materials have received considerable attention as a result of a growing need for optical sensor protection. The advance of optical detection systems for applications such as signal acquisition and night vision demands the development of protective devices, such as passive optical limiters, so that highly sensitive detectors can survive undesired high-intensity signals. Also, the ever-increasing use of lasers calls for more versatile and improved forms of eye protection. An ideal optical limiter should display the capability of being transparent at low fluences of incident light and opaque at high fluences [22]. It should also be capable of switching back and forth between these two states in quick response to external optical signals. However, most materials do not possess such an unusual property; instead, they often become more transparent under a strong light signal owing to the depletion of the electronic ground state. Silver nanoparticles, on the other hand, have been found to function as optical limiters by reverse saturable absorption. The basis of this effect is the promotion of electrons from a weakly absorbing ground state to a more strongly absorbing excited state. It has been proposed that this behavior is the result of photoinduced intraparticle charge separation leading to strong free-carrier absorption [23]. While most metal nanoparticles exhibit a weak optical limitation, it has been found to be particularly strong for gold and silver [24].

Sun et al. [23] prepared a stable suspension of silver nanoparticles and compared the optical limitation effects to similar suspensions of C_{60} and chloroaluminum phthalocyanine, which are normally considered as benchmark materials for high-performance optical limitation. The silver nanoparticles were found to be significantly more effective. This study, as well as more recent research [25, 26], shows the great potential of silver nanoparticles for use in optically limiting devices, especially if they can be effectively incorporated into transparent polymer supports [27].

1.4.4 Surface-Enhanced Raman Spectroscopy

The processes of infrared absorption and Raman scattering are routinely used in spectroscopy to detect vibrations in molecules. This can provide information on chemical structure and so helps to identify molecular structures and to determine compositions of substances and mixtures. Recent advances in instrument technology and the ability of Raman spectroscopy to examine aqueous solutions and samples inside glass containers without any preparation have led to a rapid growth in the application of the technique [28].

Raman spectroscopy relies on inelastic scattering, or Raman scattering of monochromatic light, usually from a laser in the visible, near-infrared, or near-ultraviolet range. The laser light interacts with phonons (quantized modes of vibration) resulting in the energy of the laser photons being shifted up or down. The shift in energy gives information about the vibrational modes in the system. Infrared spectroscopy yields similar but complementary information. Surface-enhanced Raman spectroscopy (SERS) uses silver or gold nanoparticles or a substrate containing silver or gold. The surface plasmon resonances of silver and gold are easily excited by the laser, and the resulting enhanced electric fields around the nanoparticles cause other nearby molecules to become Raman active. The result is amplification of the Raman signal, making it possible to detect very small concentrations of analytes. The particle enhances not only the incident laser field but also the Raman scattered field. It acts as an antenna that amplifies the scattered light intensity. The reason that the SERS effect is so pronounced is because the field enhancement occurs twice. Initially, the field enhancement magnifies the intensity of incident light that will excite the Raman modes of the molecule being studied, therefore increasing the signal of the Raman scattering. The Raman signal is then further magnified by the surface according to same mechanism, resulting in a greater increase in the total output signal of the experiment. With enhancement factors of the order of 10^{14} possible, this makes SERS an extremely sensitive spectroscopic technique to the extent that applications can extend down to single molecule detection [29]. This has created a drive to develop synthesis methods for effective metal nanoparticle-based SERS materials that can be easily applied to practical analysis.

1.4.5 Metal-Enhanced Fluorescence

Metal-enhanced fluorescence (MEF), a phenomenon where the quantum yield and photostability of weakly fluorescing species are dramatically increased, is becoming a powerful tool for the fluorescence-based applications of drug discovery, high-throughput screening, immunoassays, and protein–protein detection [30]. Fluorescence has become the dominant detection/sensing technology in medical diagnostics and biotechnology. Although fluorescence is a highly sensitive technique, there is still a drive for reduced detection limits. The detection of a fluorophore is usually limited by its quantum yield, autofluorescence of the samples, and/or the photostability of the fluorophores. However, there has been a recent upsurge in the use of metallic nanostructures to favorably modify the spectral properties of fluorophores and to alleviate some of these fluorophore photophysical constraints. The use of fluorophore–metal interactions has been termed radiative decay engineering, MEF, or surface-enhanced fluorescence [31].

Silver nanoparticles deposited on substrates have been widely used for a variety of applications in MEF typically producing >5-fold enhancements in emission intensity [31]. Metal-enhanced fluorescence is a through-space phenomenon. When fluorophores are placed within 4–10 nm of the surface nanostructures, the emission of the fluorophores is enhanced [31]. The increased emission intensity is a result of the metal nanoparticles increasing the local incident field on the fluorophore.

1.5 GENERAL SYNTHETIC STRATEGIES

The methods of producing nanoparticles are commonly separated into two main categories, “top-down” and “bottom-up” approaches.

1.5.1 Top Down

The top-down method involves the systematic breakdown of a bulk material into smaller pieces usually using some form of grinding mechanism. This is advantageous in that it is simple to perform and avoids the use of volatile and toxic compounds often found in the bottom-up techniques. However, the quality of the nanoparticles produced by grinding is widely accepted to be poor in comparison with the material produced by modern bottom-up methods. The main drawbacks include contamination problems from grinding equipment, low particle surface areas, irregular shape and size distributions, and high energy requirements needed to produce relatively small particles. Aside from these disadvantages, it must be noted that the nanomaterial produced from grinding still finds use, due to the simplicity of its production, in applications including catalytic, magnetic, and structural purposes.

1.5.2 Bottom Up

The bottom-up approach uses atomic or molecular feedstocks as the source of the material to be chemically converted into larger nanoparticles. This has the advantage of being potentially much more controllable than the top-down approach. By controlling the chemical reactions and the environment of the growing nanoparticle, then the size, shape, and composition of the nanoparticles may all be affected. For this reason, nanoparticles produced by bottom-up, chemically based and designed, reactions are normally seen as being of higher quality and having greater potential for use in advanced applications. This has led to the development of a host of common bottom-up strategies for the synthesis of nanoparticles.

Many of these general techniques can be adapted to be performed in gas, liquid, solid, or even supercritical states, hence the applicability of bottom-up strategies to a wide range of end products. Most bottom-up strategies require appropriate organometallic complexes or metal salts to be used as chemical precursors that are decomposed or reduced in a controlled manner resulting in particle nucleation and growth. One of the key differences that can be used to subdivide these strategies into different categories is the method by which the precursor is decomposed or reduced. It is beyond the scope of this book to describe all current and historical bottom-up synthetic methods of nanoparticles, as there are a great number of variations. However, as the majority of methods used involve solution synthesis based on a few well-known general techniques, the most common and applicable of these are briefly described.

1.5.3 Solution Synthesis

Scientific synthesis of nanoparticle solutions can be said to have started with experiments begun by Michael Faraday on gold in the mid-nineteenth century. Deep-red solutions of gold nanoparticles were produced by the reduction of chloroaurate $[AuCl_4]^-$ using phosphorus as a reducing agent. This is an example of chemical reduction of the metal precursor, the most common method for the generation of the nanoparticle-forming material. Other methods include thermal decomposition and photoreduction of metal ions [32–34]. For routes in which the precursor organometallic complex or metal salt is chemically reduced, this can be accomplished by using a reducing solvent such as alcohols as pioneered by Hirai and Toshima [35] or by using an added reducing agent dissolved or otherwise introduced into a nonreducing solvent. Gold nanoparticles are now routinely produced in solution, to a monodisperse particle size, by the chemical reduction of $AuCl_4^-$ by sodium borohydride in the presence of alkanethiol stabilizing agents [36]. The majority of the more straightforward approaches used for the synthesis of silver nanoparticles are based on the reduction of silver nitrate by sodium borohydride [37] or sodium citrate [38]. Other, more diverse, methods of decomposing the precursor species include microwave plasma synthesis and electrolysis of metal salts. In many nanoparticle synthesis routes, organometallic precursors play an important role by allowing more control through tailored design; that is, by selecting appropriate ligands, the solubility and decomposition rate of the precursor can be modified.

1.6 STABILIZATION

No matter how they may have been created, nanoparticles generally require some form of stabilization to prevent them from coalescing, agglomerating, or aggregating—which can detrimentally affect their properties and application. Metal oxide nanoparticles are more stable, but unprotected metal nanoparticles are subject to strong attractive forces especially at short interparticle distances. The nanoparticles are attracted together by van der Waals forces and, because of their metallic lattice structure, can easily coalesce. One method of stabilizing nanoparticles is simply to deposit, infuse, or embed the nanoparticles into a solid substrate/host material. This matrix must, of course, be suitable for the application that the nanoparticles are intended for. However, if the nanoparticles are required for synthesis or use in solution, then other techniques must be used. The two possible routes for the stabilization of nanoparticles in solution are electrostatic stabilization and steric stabilization.

1.6.1 Electrostatic Stabilization

This method is often used in the more traditional routes to nanoparticle synthesis, especially for well-controlled particle size distribution. Each metallic nanoparticle is surrounded by an electrical double layer, which causes repulsion between neighboring nanoparticles. This electrical double layer forms because of the attraction to the surface of the nanoparticle of negative ions present in the solution. These negative ions are attracted to positive metal ions at the surface of the metallic lattice of the nanoparticle. This helps to stabilize and control the growth of the forming nanoparticle. The negative ions species can be by-products of the metal feedstock (the metal salt), the reducing agent, or just species present in the solution. This coulombic repulsion between the particles caused by the electrical double layer formed by ions adsorbed at the particle surface (e.g., sodium citrate) and the corresponding counterions is exemplified by gold

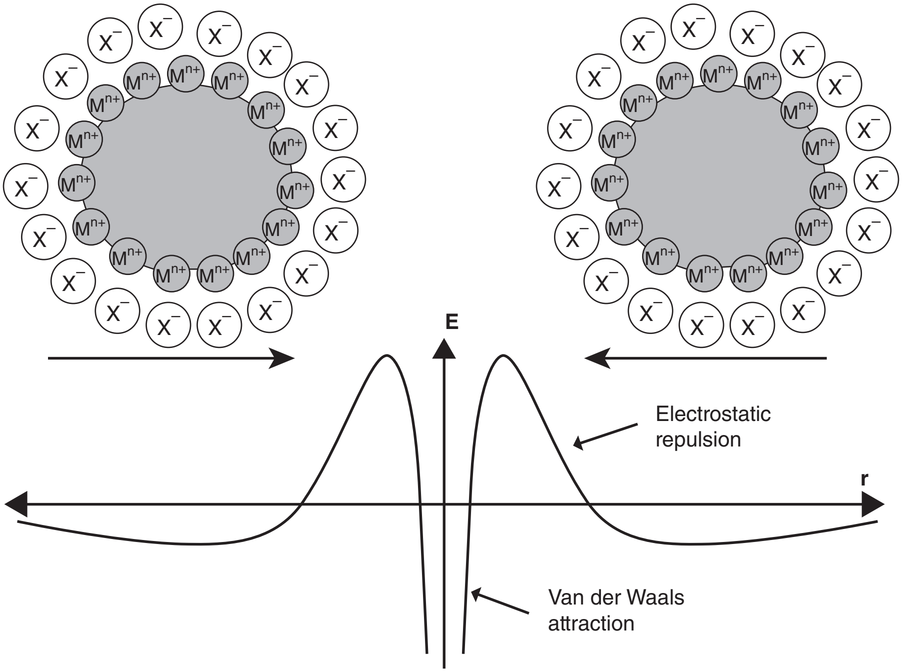

Figure 1.4. Electrostatic stabilization of metal nanoparticles. Attractive van der Waals forces are outweighed by repulsive electrostatic forces between adsorbed ions and associated counterions at moderate interparticle separation.

sols prepared by the reduction of $[AuCl_4]^-$ with sodium citrate [39]. See Figure 1.4 for a schematic representation of this process.

1.6.2 Steric Stabilization

Steric stabilization is achieved by the coordination of sterically demanding molecules such as polymers, surfactants, or ligands that act as protective shields on the metallic surface. In this way, nanometallic cores are separated from each other and agglomeration is prevented [40] (see Fig. 1.5). This can occur because of the electron-deficient nature of the metal surface. Metal ions in the bulk of a lattice are commonly surrounded on all sides by the delocalized electrons in the structure. This leaves the metallic ions on the lattice surface, especially the curved surface of a nanoparticle, comparatively electron deficient. Therefore, it is necessary for steric protecting agents to have suitable electron-donating groups. These groups coordinate to the surface of the metal nanoparticle.

The main classes of protective groups are polymers and block copolymers, usually with P, N, O, and S donors (e.g., phosphanes, amines, esters/ethers, thioethers), or solvents such as tetrahydrofuran and methanol that have electron-rich groups. The steric protecting agent, in order to function effectively, must not only be attracted to the nanoparticle surface but also be adequately solvated by the dispersing fluid.

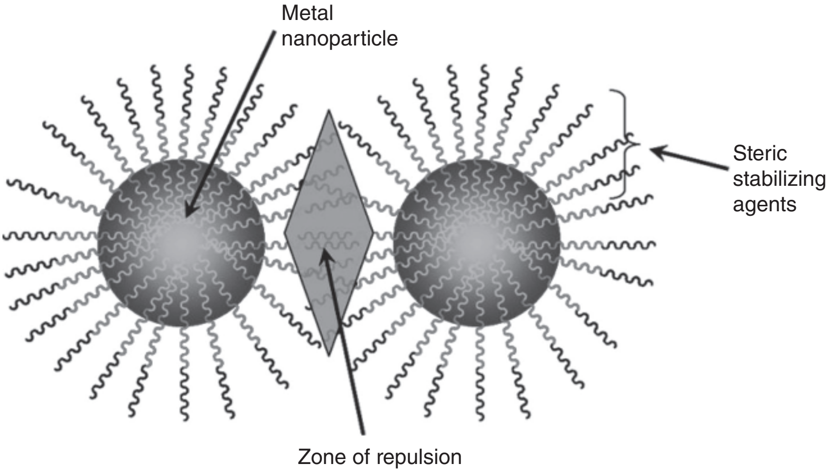

Figure 1.5. Steric stabilization of nanoparticles. Stabilizing agents may be uniform or may be composed of different segments to provided separate functions, for example, a nanoparticle-philic segment and a solvent-philic segment.

1.7 POLYMERS

From the earliest recorded times, man has exploited naturally occurring polymers as materials for providing clothing, shelter, and tools. Nowadays synthetic polymers have considerable commercial importance and have become an integral part of our daily lives. From the developments of the first commercial synthetic polymers in the early twentieth century to today, the breadth of polymer science has been ever increasing, and regular advances have continued to stimulate both scientific and industrial progress. The use of polymeric materials is increasing rapidly year by year as polymers are tailored to replace conventional materials such as metals, wood, and natural fibers. The degree to which polymer properties can now be adapted and controlled by modification of chemical structure, the blending of polymers, or the production of unique architectures has led to polymeric materials being designed to fill new and specific roles that no other known material could provide. It is because of this need for new functional materials that the development of polymeric materials has become combined with the emergent field of nanotechnology via the incorporation of nanomaterials into polymers to produce novel hybrid materials.

1.7.1 Definition

Polymers are large molecules made up of repeating units. They are synthesized from simple monomer molecules. These monomers become linked together forming chains increasing in size from dimers and trimers to oligomers and eventually polymers with a molecular weight of at least several thousand atomic mass units or more. By changing from a monomeric to a polymeric structure, the nature of the material is greatly altered.

While the monomeric substance may have been naturally liquid or even gaseous, it will become a solid or at least a viscous liquid as a polymer. This is because the polymeric chains become entangled with each other, their molecular forces of attraction to each other are greatly compounded, and the timescale of movement of the repeating units is severely retarded. It is useful to describe some general features of polymers here, such as crystallinity and glass transition. The production of metal nanoparticle–polymer composites will also be given a general overview.

1.7.2 Crystallinity in Polymers

The long chains that make up the structure of the polymers exist in one of two possible arrangements:

- Amorphous—chains form a randomly ordered, chaotic "mess" (like a plate of spaghetti).
- Crystalline—chains are arranged in an ordered manner (like dry spaghetti in a packet).

It is normal for these arrangements to coexist in the bulk of a polymer, with the proportions of each depending on the polymer in question. Most polymers are therefore described as semicrystalline (Fig. 1.6).

Crystallinity makes a polymer denser, more resistant to solvents, and more opaque (the crystallites scatter light). The mechanical properties of a polymer are also affected by its crystallinity as well as the position of its glass transition temperature.

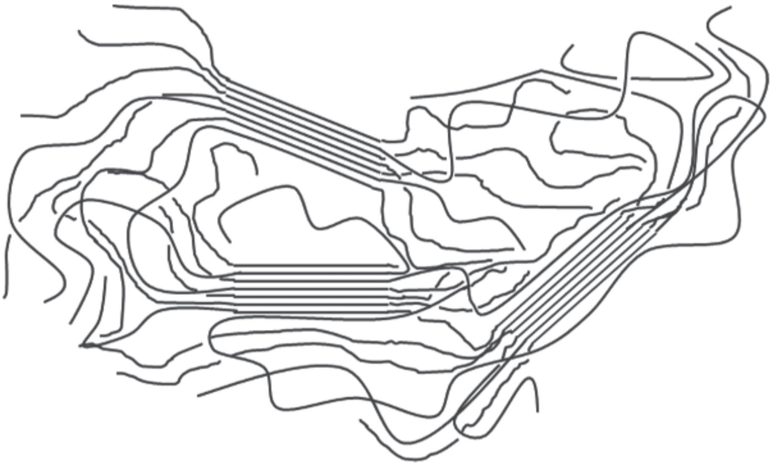

Figure 1.6. Schematic of semicrystalline polymer showing ordered crystallites separated by amorphous areas.

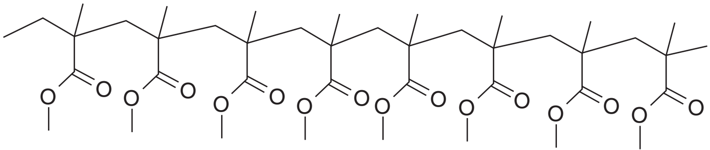

Isotactic PMMA

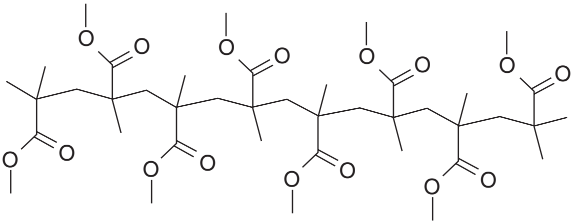

Syndiotactic PMMA

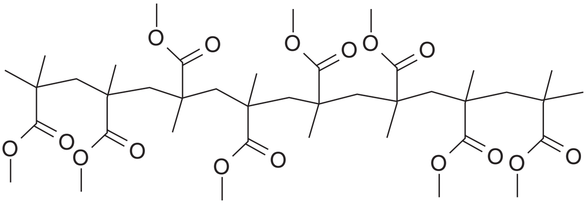

Atactic PMMA

Figure 1.7. Possible tacticities of PMMA. Which tacticity is formed is governed by the method of polymer preparation. The free radical polymerization mechanism most commonly used allows no control over the position the side group takes and so produces atactic PMMA.

Poly(methyl methacrylate) (PMMA) provides a good example for discussing how the structure of the individual polymer chains of a polymer can determine the crystallinity of the material. When PMMA has an atactic structure (Fig. 1.7), the lack of order of the side groups prevents the chains from being able to pack together effectively, leading to a disordered, amorphous material. Isotactic PMMA, alternatively, is quite crystalline. Its ordered structure allows the polymer chains to effectively pack together into crystallites.

1.7.3 The Glass Transition and Melting Point

The glass transition occurs at a specific temperature, T_g, that is different for each polymer. Below the glass transition temperature, the polymer is hard and brittle (like glass); above, it is softer and more flexible (like rubber). This glass transition is very different to melting. Melting (T_m) occurs in the crystalline part of polymers, when rigid chains in the crystals loosen, becoming a disordered liquid. The glass transition is something inherent to only the amorphous region. It is therefore normal for polymers to have both a T_g and a T_m if they possess amorphous and crystalline parts.

The position of the T_g is very important in polymer engineering and use. It governs how easy they are to process and what use they can be put to. Whether a polymer's T_g is above or below room temperature, or close to it, will affect the possible end applications of the material. This transition is related to the amount of mobility that the polymer chains possess. Below the T_g the chains have relatively little scope for free movement, though the segments are still moving and rotating a good deal. Above the T_g the chains have gained a greater mobility, and their thermal energy causes increased movement, creating more free volume for the polymer chains to slide past each other more easily. Because of this, if a force is applied to a polymer that is above its T_g, the chains are able to move to relieve the stress, and the polymer bends. If a force is applied to a polymer that is below the T_g, the chains will be unable to move in this way, and the polymer will either resist the force or break.

1.8 METAL–POLYMER NANOCOMPOSITES

The embedding of nanoscopic metals into dielectric matrices represents a solution to manipulation and stabilization problems. For functional applications of nanoparticles, polymers are particularly interesting as an embedding phase since they may have a variety of characteristics: they can be an electrical and thermal insulator or conductor, may have a hydrophobic or hydrophilic nature, can be mechanically hard (plastic) or soft (rubbery), and so on. Finally, polymer embedding is the easiest and most convenient way for nanostructured metal stabilization, handling, and application. This has fuelled investigation into the preparation of metal–polymer nanocomposites. These composites most commonly take the form of thin polymer films or powders, as this is normally the simplest structure to prepare and also good for exploiting the desired properties. Preparation techniques can be classified as *in situ* and *ex situ* methods. In the *in situ* methods, the monomer is polymerized, with metal ions introduced before or after polymerization. Then the metal ions in the polymer matrix are reduced chemically, thermally, or by UV irradiation, to form nanoparticles. In the *ex situ* process, the metal nanoparticles are synthesized first, and their surface is organically passivated. The derivatized nanoparticles are then dispersed into a polymer solution or liquid monomer that is then polymerized. A more detailed description of some of these key techniques follows.

1.8.1 *Ex Situ*

The metal nanoparticles are prepared first, traditionally by the controlled precipitation and concurrent stabilization of the incipient colloids. This can be done by the reduction of a metal salt dissolved in an appropriate solvent, often containing a polymer stabilizer. Alternatively, it can be prepared by controlled micelle, reverse micelle, or microemulsion reactions. The particles produced by these methods are often surface modified to prevent aggregation, either covalently by metal–thiol bonds [41] or by coating with a suitable polymer shell [42]. These particles then need to be introduced into polymers. This is accomplished by mixing with a solution of the polymer, or monomer, which can then be spin cast according to standard polymer processing techniques. However, this method is limited by problems of dispersion. It is necessary to surface modify the particles, therefore altering their properties, in order to disperse them. Even with this step, it is difficult to produce well-dispersed composites, and a certain degree of aggregation remains. Also, this route is limited to compatible polymer–particle–solvent systems.

1.8.2 *In Situ*

The *in situ* methods that have been used for the manufacture of metal nanoparticle–polymer composites consist of much more varied techniques. *In situ* methods, though often less simple and straightforward as *ex situ*, are commonly considered to produce better quality and more controlled nanocomposite materials. An outline of the most significant methods follows.

1.9 THERMAL DECOMPOSITION OF METAL PRECURSORS ADDED TO POLYMERS

This represents the existing method most suited to large-scale production. A number of organic precursors were studied for this application without showing completely satisfying behavior until it was discovered that homoleptic mercapeptides (i.e., $M_x(SR)_y$) are effective in the production of metal–polymer nanocomposites [43]. Transition metal mercapeptides are covalent organic salts with a high compatibility with most hydrophobic polymers. The mercapeptide is dispersed in a polymer, and the polymer is then heated to 110–180 °C to decompose the mercapeptide. This produces zerovalent metal or metal–sulfide nanoparticles, depending on the metal and conditions. The literature also reports similar interesting composites prepared by the inclusion of metal nitrates (e.g., $AgNO_3$) [44–47] and metal salts (e.g., $HAuCl_4$) [48]. In these methods organic by-products are left trapped in the polymer, and the reduction of the metal causes damage to the substrate by electron extraction. With any nanocomposites produced by this method, the precursors must be included in the polymer *before* it is cast into a solid form. Any subsequent processing may then damage or affect the composite.

1.10 ION IMPLANTATION

An ion beam (e.g., Ag^+) of the range 30–150 keV in energy is directed at the surface of a polymer sample. As the ions enter the matrix, nuclear collisions occur, displacing atoms in the polymer matrix and breaking some of its chemical bonds. Along with this, target atoms effectively lose electrons, and the implanted M^+ ions deionize with the formation of neutral metal atoms (M^0). It is possible in principle for metal atoms to combine with organic radicals and polymer ions. However, because of the great difference in Gibbs free energy between metal atoms and atoms of the polymer, metal–metal bonding is energetically more favorable. Though offering good control of particle size and dispersion, this method is limited to impregnating a few micrometers into the surface. Also, it can lead to the formation of carbonized shells around the metal nanoparticles. Nevertheless, it has been used for the effective synthesis of metal–polymer nanocomposite materials including PMMA–Ag nanocomposites [49, 50].

1.11 CHEMICAL VAPOR DEPOSITION (CVD) AND PHYSICAL VAPOR DEPOSITION (PVD)

These methods, though consisting of many subdivisions, involve the formation of a solid from a controlled deposition of gaseous species. Both processes are commonly used, especially in the electronics industry, for coating materials with thin films but have also been used to produce nanoparticles. Due to the nature of these processes, the nanoparticles are commonly deposited onto a suitable substrate, such as an inorganic support, or with a co-deposited polymer.

Chemical vapor deposition (CVD) is a chemical process used to produce high-purity, high-performance solid materials. In a typical CVD process, the substrate is exposed to one or more volatile precursors, which react and/or decompose on the substrate surface to produce the desired deposit. Frequently, volatile by-products are also produced that are removed by gas flow through the reaction chamber. The precursors used are volatile organometallic complexes, similar to those sometimes used in the synthesis of nanoparticles through solution methods. In CVD, precursor gases (often diluted in carrier gases) are delivered into the reaction chamber at approximately ambient temperatures. As they pass over or come into contact with a heated substrate, they react or decompose forming a solid phase that is deposited onto the substrate. Okumura et al. used this technique to form catalytic nanoparticles of gold on inorganic substrates [51].

Physical vapor deposition (PVD) is similar but allows the nanocomposite films to be generated more simply from the pure material/materials intended to form the nanoparticles/composite. This is achieved by thermal evaporation (by an electron beam or resistive heating) of the starting materials to form a vapor phase. A carrier gas is then introduced to transport the evaporated metal away from the heater, towards the cool end of the reactor. As the vapor cools, nucleation occurs and liquid metal droplets form. These droplets collide, coalesce, and solidify in a manner controlled by the temperature gradient, residence time, and gas flow rates employed during the procedure. This is preferable to CVD as it produces no by-products. Oxygen is frequently used as a carrier gas in order to produce metal oxide particles.

When these methods are used for the simultaneous synthesis of metal nanoparticles and a polymer substrate, this forms the nanoparticles inside the polymer substrate with a good deal of control on the structure of the composite produced being possible. By controlling the flows of the two feedstocks, the nanocomposite can be made continuous, gradated or layered, etc.

1.12 $\mathrm{scCO_2}$ IMPREGNATION INTO POLYMERS

Supercritical fluid (SCF) methods for the generation of metal nanoparticles in solid polymers, by infusing precursor complexes subsequent to their reduction, are outlined in the following section. The advantages of the $\mathrm{scCO_2}$ method are many. It is a green process, avoiding the use of toxic and harmful solvents as well as the problems of their removal. It allows the modification of polymers that are difficult to process by normal methods. It has promising potential for effective and economical scale-up. Importantly, it allows the production of pure, non-surface-coated nanoparticles, without leaving any trapped by-products in the polymer. It would also allow prefabricated polymeric materials to be impregnated with nanoparticles after they had been processed into their final form, which avoids detrimental aggregation of the nanoparticles during processing.

1.13 SUPERCRITICAL FLUIDS

1.13.1 The Discovery and Development of SCFs

Supercritical fluids are useful because they possess both liquid-like and gas-like properties. The critical point of a substance was first discovered and defined by *Baron Charles Cagniard de la Tour* in 1822. His experiments proved the existence of SCFs by heating various solvents sealed within metal cannons. By observing the changes in solvent acoustics, *de la Tour* was able to identify the existence of a *new* single phase, rather than the two separate liquid and gas phases [52].

This initial discovery sparked subsequent investigations, and in 1869 Dr. Thomas Andrews reported the critical parameters of carbon dioxide and illustrated the phases by constructing the first supercritical phase diagram [53]. In 1879, at a *Royal Society* meeting, *Hannay* and *Hogarth* reported the ability of certain compressed gases to dissolve salts such as cobalt chloride, potassium iodide, and potassium bromide, which was previously thought to be impossible [54]. In summary:

> We have the phenomenon of a solid dissolving in a gas, and when the solid is precipitated by reducing the pressure, it is brought down as a "snow" in the gas or on the glass as a "frost," but it is always easily redissolved by the gas on increasing the pressure (326).

These initial investigations lead on to further work and the eventual definition of an SCF, by Darr and Poliakoff, as "*any substance, the temperature and pressure of which are higher than their critical values, and which has a density close to or higher than its critical density*" [55]. This is best explained with reference to a phase diagram (Fig. 1.8). Similar to gases, SCFs possess high diffusivities, important for reaction kinetics, while also having liquid-like densities that allow them to act as effective solvents for many compounds. Small changes in pressure and temperature can be used to "tune" the density of an SCF and therefore its solvating ability, hence giving increased control of reactions.

Supercritical fluids are unique solvents with a wide range of interesting properties. They can be clean and versatile, capable of processing a wide variety of materials. An increasing drive for greener processes in chemistry and industry in the 1970s led to a move towards the wider use of SCFs as alternative reaction media, for example, for extraction and separation processes. This marked the need for a move away from volatile organic compounds and ozone-depleting substances such as chlorofluorocarbons, which are often used as processing solvents. Many of these traditional solvents are not only environmentally harmful but often hazardous and toxic to humans, with high costs of waste removal.

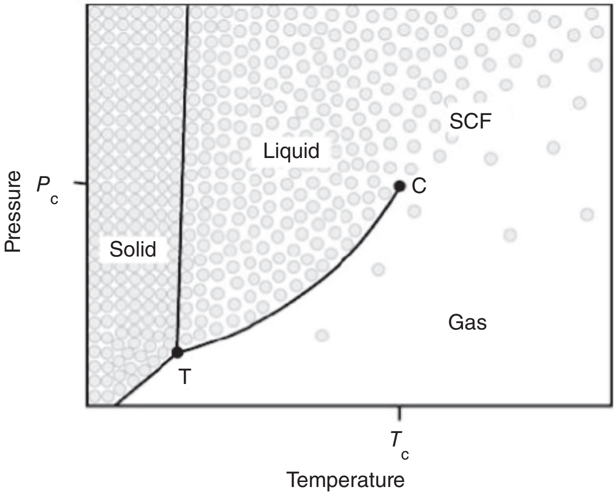

Figure 1.8. Schematic pressure–temperature phase diagram for a pure component showing the SCF region. The triple point (T) and critical point (C) are marked. The circles show the density variation of the substance in the different regions of the phase diagram. Note that the density varies continuously between the liquid state and the gas state, provided that the liquid–gas equilibrium line is not crossed [56]. Reproduced by permission of The Royal Society of Chemistry.

1.13.2 Supercritical CO_2

CO_2 in particular has received much attention as an SCF and is probably the most widely used. The choice of which SCF is used for chemical and industrial processes must be determined by a compromise of practical factors. Supercritical processes have associated costs arising from the need for high-pressure equipment, and therefore solvents with more easily reached critical points will lower this cost, but this must be offset by the financial cost of the solvent, ease of handling, solvent reactivity, and safety factors.

CO_2 has relatively easily accessible critical points of 31.06 °C and 1070 psi (7.38 MPa) and tunable density, as well as a high diffusivity, making it a promising reaction medium for organic compounds. There are of course other substances that share these properties. However, many of them have considerable disadvantages not present for $scCO_2$. Most of the organic solvents suitable for supercritical applications are flammable, often dangerously so. They also tend to have potentially harmful effects to health and the environment. CO_2 is noncombustible and nontoxic as well as being relatively environmentally benign. It is also easily available as it is naturally occurring as well as being the by-product of many industrial processes, such as the burning of fossil fuels for power. As a consequence of this, both high-quality and low-quality stock can be easily obtained, meaning that CO_2 is relatively inexpensive and financially desirable as a reaction medium. Water also shares some of these advantages of nontoxicity and availability. However, high critical parameters and corrosion problems with metal equipment impede its wider application.

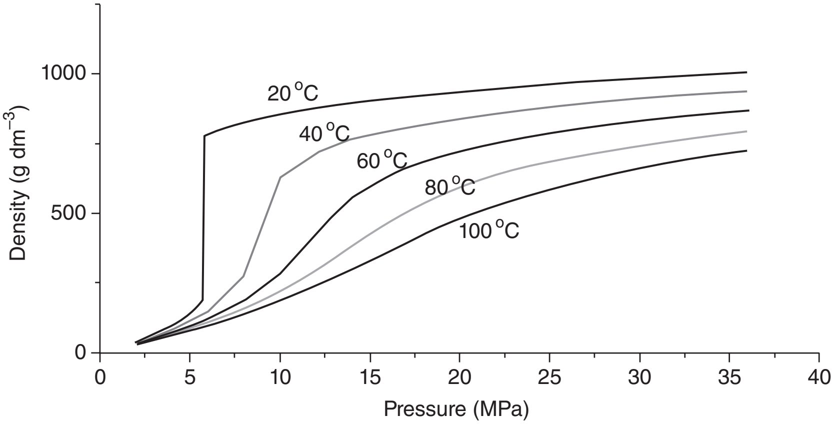

Figure 1.9. The density of CO_2 as a function of pressure for a range of temperatures.

As CO_2 is a gas at ambient temperatures and pressures, it can be easily removed, leaving no solvent residues in the processed material. The ease of its removal contrasts with the high energy costs of drying for the removal of conventional solvents. In small-scale reactions, the CO_2 contribution to greenhouse effects will be negligible, but for larger-scale processes, CO_2 can be recycled back into the reaction system.

The density of $scCO_2$ in a range of temperatures and pressures is shown in Figure 1.9. It is this easily tunable density, and consequently solvent strength, that allows facile control of reactions and processes.

Many of the processes for which $scCO_2$ is used are aided by zero surface tension, allowing hydrophobic behavior normally associated with liquid to substrate interactions, and other phenomena such as drying-induced substrate damage, to be avoided. This has allowed $scCO_2$ to be utilized as an ideal solvent for the cleaning and processing of delicate electronic components and micro-devices. As well as use in microelectronics, $scCO_2$ has found widespread application in other industrial processes, such as the extraction of metals or organic material. CO_2 has also been used for foodstuffs, notably extracting caffeine from coffee, and also for dry cleaning and degreasing. CO_2 is even being employed in increasingly large scales for organic synthetic reactions and transformations [57–59]. However, the two aspects of $scCO_2$ use most relevant to the scope of this book are the processing and synthesis of polymers, and $scCO_2$ generation and impregnation of nanoparticles. These topics will be discussed in greater detail later.

1.14 POLYMER PROCESSING WITH $scCO_2$

The solvating ability of $scCO_2$ when interacting with polymers has been compared to volatile organic solvents, such as hexene. The density of $scCO_2$, as governed by its temperature and pressure, affects its solvent nature, which is commonly measured by dielectric constant. While a good solvent for many polar and nonpolar molecules of low molecular weight (e.g., monomers, initiators, oligomers), $scCO_2$ is a poor solvent for most high-molecular-weight polymers [56]. The solubility of polymers in scCO$_2$ is governed by the CO$_2$–polymer segment interactions, compared to the strength of the segment–segment and CO$_2$–CO$_2$ interactions, and the flexibility of the polymer chain [60]. As a quadrupolar molecule, CO$_2$ does not strongly interact with nonpolar groups and hence, combined with having a lower density than most liquid solvents, is a poor solvent for many long-chain polymers. Solubility in scCO$_2$ generally increases with the number of polar groups in the polymer [61]. However, for very polar polymers, segment–segment interactions will be too strong, therefore reducing solvation.

The factors that control polymer segment–CO$_2$ interactions are not yet fully understood. Fluorine-functionalized polymers have been widely investigated, as they seem to have a greater affinity for CO$_2$. However, this appears to be linked to carbonyl/ether groups present in the polymers, which are generally accepted to have a favorable interaction with CO$_2$. It is noted that poly(tetrafluoroethylene) (PTFE), completely fluorinated as it is, though with no carbonyls/ethers, is no more miscible with scCO$_2$ than a polyolefin. Three important features that help in making a polymer scCO$_2$ soluble are:

1. Low cohesive energy
2. High free volume
3. Groups that provide a specific interaction with scCO$_2$, that is, F, C = O, ether etc.

For polymers that are soluble, or semi-soluble, scCO$_2$ can be used for the extraction of low-molecular-weight material, as well as polymer fractionation. Polymerization reactions have been successfully carried out in scCO$_2$, often with surfactants or cosolvents to aid solubility or dispersion of higher-molecular-weight species [56, 62, 63]. These reactions are capable of producing easy to process particulate powders of solid polymer, and there are numerous publications in the literature where scCO$_2$ has been used as a solvent to facilitate clean polymer synthesis [62, 64–73]. Much of this research has centered on the ability to develop CO$_2$-soluble polymer segments, to stabilize the growing polymer chain, enhance its dispersion in scCO$_2$, and ensure controllable, reproducible polymer preparations.

Insoluble polymers have received at least as much attention for use with scCO$_2$. Even though they are not soluble in scCO$_2$, it is still able to permeate into them, leading to some very useful effects. Even a small amount of scCO$_2$ absorbed into a polymer phase results in substantial and sometimes dramatic changes in the physical properties that dictate processing. These include viscosity, permeability, interfacial tension, and glass transition temperature. The permeation of scCO$_2$ into a polymer causes it to swell in volume. The CO$_2$ molecules, aided by their zero surface tension, permeate easily into a polymer matrix, allowing the chains a greater mobility. The CO$_2$ molecules act as "molecular lubricants" between the chains, giving them more free volume of movement and therefore reducing the T_g. This also gives the polymer chains the freedom to align themselves into a more favorable order, hence increasing crystallinity.

The permeation of scCO$_2$ into polymers has been used for extraction, foaming, and impregnation. Extraction occurs by simply removing the soluble extractant material, such as unreacted monomer, while leaving the insoluble substrate. Foaming occurs when rapid decompression forms gaseous CO$_2$ inside the polymer. As for impregnation, by utilizing its properties as a transport medium, molecules can be dissolved in $scCO_2$, impregnated into a polymer, and CO_2 can be cleanly removed afterwards. Substances impregnated into polymers have included dyes, fragrances, drugs for controlled release, antimicrobial and antifungal agents, and metal nanoparticles [74]. The impregnation technique has also led to a novel method of producing polymer blends by introducing a monomer before initiating polymerization.

1.15 NANOPARTICLES BY $scCO_2$ IMPREGNATION OF HOST MATERIALS

Supercritical fluids have been used to deposit thin metal films onto a wide range of surfaces and to incorporate metallic particles into different inorganic and organic substrates for microelectronic, optical, and catalytic applications [75]. This technique has allowed both highly dispersed and uniformly distributed metal nanoparticles and agglomerated clusters of nanoparticles of wider size distribution to be generated in host materials. These various solid substrates have included silicon wafer, metal foil, inorganic nanotubes, bulk polymers and polymer membranes, and organic and inorganic porous materials. The nanoparticle impregnation process involves dissolving an appropriate metallic precursor in an SCF (most commonly $scCO_2$) and then exposing the substrate to the solution. The SCF facilitates the infusion of the precursor into the host material. After incorporation of the precursor with the substrate, the metallic precursor is reduced to its metal form by a wide variety of methods resulting in films or particles. The reduction methods employed are chemical reduction in the SCF with a reducing agent such as hydrogen and alcohols, thermal reduction in the SCF, and thermal decomposition in an inert atmosphere or chemical conversion with hydrogen or air (Fig. 1.10).

The use of an SCF such as $scCO_2$ for this impregnation process is advantageous in comparison to conventional solvents for many reasons. For many of the substrates used, a conventional solvent would be unsuitable. For high-surface-area substrates such as highly porous inorganics for catalysis or microstructured materials for electronics, the use of conventional solvents is not appropriate. The surface tension and viscosity of common solvents, along with poor wetting of the pores, cause very slow and often incomplete impregnation of precursor solutions into porous supports. The low surface tension of $scCO_2$ not only permits better penetration and wetting of pores than liquid solvent but also avoids pore collapse that can occur on certain structures such as organic and silica aerogels with liquid solvents. This damage is caused during the drying step, as liquid solvents are removed from the substrate. Strong localized forces occur in the pores due to their small diameter in relation to the meniscus of retreating liquid. This causes cracking of the material. Even without this factor, extended heating of the substrate to remove liquid solvents can be costly and time consuming. In comparison, $scCO_2$ can be much more easily introduced and removed from such systems.

For polymer impregnation $scCO_2$ allows modification that would be difficult with conventional solvents. $scCO_2$ can be easily infused into polymers, without the need to dissolve the polymer and reblend, and displays a high permeation rate in virtually all polymers. The exposure of polymers to $scCO_2$ results in various extents of swelling and

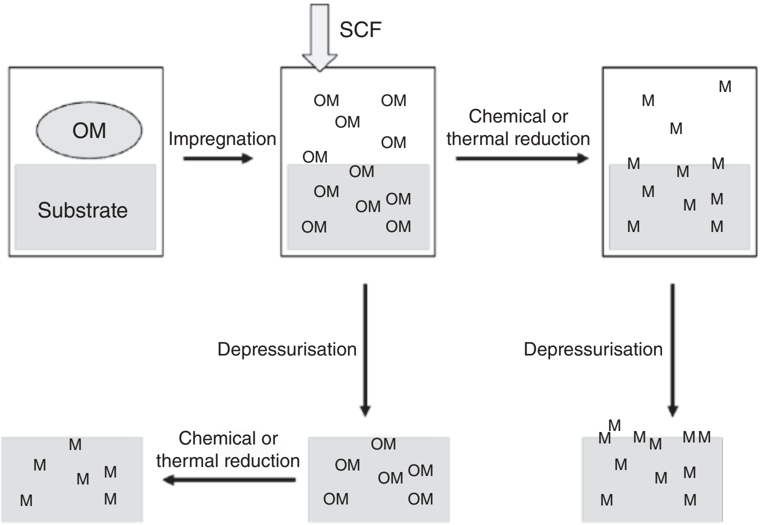

Figure 1.10. Supercritical fluid-mediated impregnation or deposition of nanoparticles into a substrate. OM represents a soluble organometallic precursor. Adapted from Reference [75]. Copyright 2006, with permission from Elsevier.

enhanced mobility of the polymer chains, which makes it possible to incorporate metallic precursors. The infusion of $scCO_2$ causes a lowering of the T_g of the polymer, allowing easier processability and molecular infusion. Moreover, the degree of polymer swelling, diffusion rates within the substrate, and the partitioning of precursors between the SCF and the swollen polymer can be controlled by density-mediated adjustments of solvent strength via changes in temperature and pressure [75, 76].

Regardless of the substrate used, the gas-like diffusivities of $scCO_2$ significantly enhance the kinetics of penetrant absorption, and no solvent residues are left after depressurization. The average particle size and size distribution of nanoparticles are affected by the precursor reduction method used, as well as the conditions, type, and amount of precursor in the system and the surface properties of the substrate.

The groundbreaking work in this field was undertaken by Watkins and McCarthy in 1995 and was the first use of an SCF for the impregnation of metal nanoparticles into a polymer substrate [76]. In this case the SCF used was $scCO_2$ and the polymers impregnated were poly(4-methyl-1-pentene) (PMP) and PTFE. The organometallic precursor used was dimethyl(cyclooctadiene)platinum(II) ($CODPtMe_2$), which was chosen because it was a readily available CVD precursor with good potential for $scCO_2$ solubility and had previously been reduced effectively with hydrogen to yield high-purity platinum films [77]. The precursor was infused into the polymers by a 4 h impregnation time in $scCO_2$ at a temperature of 80 °C and pressure of 15.5 MPa. The precursor was reduced to platinum nanoparticles in the PMP by hydrogen reduction in $scCO_2$, hydrogen reduction after depressurization, and thermal decomposition in the presence of $scCO_2$. In PTFE the precursor was reduced by hydrogen in the presence of $scCO_2$. The results

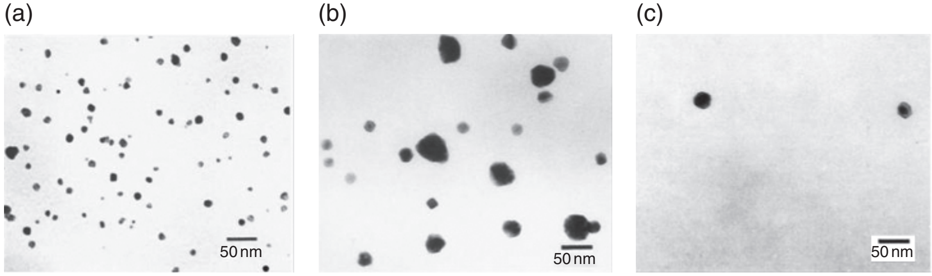

Figure 1.11. (**a**) Poly(4-methyl-1-pentene), hydrogen reduction after depressurization. (**b**) Poly (4-methyl-1-pentene), hydrogen reduction in the presence of $scCO_2$. (**c**) Poly(tetrafluoroethylene), hydrogen reduction in the presence of $scCO_2$. Reproduced with permission from Reference [76]. Copyright 1995 American Chemical Society.

of these impregnation reactions provide a useful example to discuss the effect of changes in the system and can be observed from transmission electron micrographs of the nanocomposites (Fig. 1.11).

The comparison of Figure 1.11a and b is useful for understanding the implications of the two alternative reduction routes shown in Figure 12, that is, reduction after or before depressurization. When the precursor in PMP was reduced after depressurization of the $scCO_2$ (Fig. 1.11a), the product appeared to be homogeneous throughout with nanoparticles of ~15 nm evenly distributed, apart from occasional larger clusters. When the precursor was reduced by hydrogen before venting the $scCO_2$, a sharp concentration gradient was seen close to the surface. The nanoparticles in the bulk of the PMP are mostly up to ~50 nm. However, close to the surface, which had a silver sheen, there was a greatly increased concentration of nanoparticles with diameters of ~50–100 nm. This difference is caused by the effect of reducing the metal while $scCO_2$ is still present in the polymer. The polymer is still $scCO_2$ swollen, and the precursor molecules are still able to diffuse freely during the reduction step. This allows the nanoparticles in the bulk to grow larger in diameter and also caused a greater deposition of metal into the surface layer. This is because the precursor is still able to infuse from the solvent phase into the polymer and because metal nanoparticles growing in the solvent phase will become unstable and deposit into the polymer surface. Therefore, when control of nanoparticle size and uniformity is desired, post-depressurization reduction is preferable.

We should also compare the difference in nanocomposite structure produced depending on the change of host polymer. Poly(tetrafluoroethylene) was impregnated with precursor that was reduced in the presence of $scCO_2$ (Fig. 1.11c) in exactly the same method as the PMP (Fig. 1.11b). A similar surface effect was noticed for the PTFE, compared to the PMP, in terms of there being more and larger nanoparticles at the polymer surface due to reduction occurring concurrently with impregnation. However, in the case of PTFE, the nanoparticles in the bulk of the polymer were considerably fewer in number and smaller in size than those produced in PMP in the same conditions. This demonstrates that although $scCO_2$ can be used to impregnate even very solvent-resistant polymers such as PTFE, the degree of nanoparticle incorporation is understandably affected by the uptake of precursor and this is determined by the solubility of the precursor in each given polymer and how easily the precursor can be infused into the polymer.

This method was expanded by Watkins' group to deposit different metal nanoparticles or films, including platinum, palladium, gold, rhodium, cobalt, nickel, and copper in $scCO_2$ by the reduction of desired precursors with hydrogen or alcohols [78–83]. Other groups then took this new technique forward, adapting it to other substrates and metals. Ye et al. prepared highly dispersed nanoparticles of palladium, rhodium, and ruthenium through reduction of adsorbed metal-β-diketone precursors by hydrogen in $scCO_2$ [84–87]. The nanoparticles were deposited onto functionalized multi-walled carbon nanotubes or SiO_2 nanotubes for catalytic applications. Preliminary experiments demonstrated that the supported Pd nanoparticles were effective catalysts for hydrogenation of olefins in carbon dioxide showing high electrocatalytic activity for oxygen reduction reaction indicative of potential fuel cell applications.

Saquing et al. demonstrated that metal films and highly dispersed nanoparticles could be produced simultaneously on the surface and within the matrix of porous monolithic materials by depositing platinum on carbon aerogel monoliths [88]. Further research led by Saquing and Erkey's group continued this work to other substrates including carbon black, silica aerogel, silica, gamma-alumina, and Nafion® 112 film [89]. Nafion® is a sulfonated tetrafluoroethylene copolymer developed by DuPont. The porous substrates and Nafion® film were impregnated with $CODPtMe_2$, which was reduced to elemental platinum by heat treatment in the presence of nitrogen gas. A comparison of nanocomposites produced under different conditions showed that both the metal contents and the particle sizes are controllable. Membrane–electrode assemblies of Nafion® membranes with incorporated palladium nanoparticles were prepared by this method and evaluated in direct methanol fuel cells. The Pd-impregnated Nafion® membranes showed reduced methanol crossover and gave higher cell performance than that of pure Nafion® membrane.

Substantial investigations into this field have been undertaken by the Howdle group at the University of Nottingham. The method used by the Howdle group has been generally similar to that commonly used, except instead of reducing the metallic precursor at ambient pressure following SCF impregnation, chemical reduction with pure hydrogen at an elevated pressure was used to synthesize silver nanoparticles in porous poly(styrene-divinylbenzene) beads and silica aerogels and palladium nanoparticles in silica aerogel [90, 91]. The palladium nanoparticles in silica aerogel supports were shown to demonstrate good catalytic activity for hydrogenation of cyclohexene in a continuous flow reactor. Similar impregnations allowed the clean synthesis of silver nanoparticles in polymer substrates for biomedical applications, and some success was demonstrated in initial applications testing [92, 93]. More recently the group was able to extend the versatility of this technique to the synthesis of gold nanoparticles supported on silica, polyamide, polypropylene, and PTFE [94]. Two precursors, dimethylacetylacetonate gold(III) and its fluorinated analogue dimethylhexafluoroacetylacetonate gold(III), were compared for their effectiveness in the production of the gold nanoparticles, which have catalytic applications. Interestingly the non-fluorinated organometallic precursor was found to produce more effectively and higher loaded nanocomposite material.

Some of the most advanced polymer results are evidenced by the researches of Boggess et al. and of Yoda et al. Boggess et al. performed the synthesis of highly reflective silver–polyimide films by impregnation of (1,5-cyclooctadiene)(1,1,1,5,5,5-hexafluoroacetylacetonate)silver(I) into polyimides [95]. Similarly, Yoda et al. synthesized Pt- and Pd-nanoparticle-dispersed polyimide films as a precursor for the preparation of metal-doped carbon molecular sieve membranes for hydrogen separation [96]. The impregnated precursors were Pt(II) acetylacetonate and Pd(II) acetylacetonate. It was found that the particle size increased with the increase of the impregnation temperature and impregnation time. The Pd-doped carbon molecular sieve membrane was successfully prepared by carbonation of the Pd-doped film and showed good hydrogen separation performance [97]. Yoda et al. also prepared platinum/silica aerogel nanocomposites by dissolving platinum(II) acetylacetonate in $scCO_2$ and impregnating into the silica gel during the supercritical drying stage [98].

These initial investigations into the use of $scCO_2$, though interesting and successful, only represent the beginning of research that will bring this exciting field into full understanding and effectiveness, but there is clearly a great potential for creating hybrid materials with improved properties.

The first section of this chapter has outlined the importance of the emergent field of nanocomposite functional materials and that the development of new routes to metal–polymer nanocomposites is a relevant and necessary area of research. Supercritical fluid technology has been explained as a useful technique with many advantages over conventional solvents.

This second half of the chapter gives some specific examples of how $scCO_2$ has been used to prepare metal nanoparticle-loaded polymer materials. The synthetic routes are outlined and the applications of these materials are discussed. These examples have been chosen to indicate the wide scope such materials may find use in, with fields covering optical/photonic sensors, antimicrobial medical materials, gas uptake, and catalysis.

1.16 SYNTHETIC METHOD FOR IMPREGNATING POLYMER FILMS WITH METAL NANOPARTICLES

The main criteria for choosing metal precursor complexes include solubility in $scCO_2$, affinity to polymer host, and decomposition temperature. The most commonly used silver precursor, for example, is (1,5-cyclooctadiene)(1,1,1,5,5,5-hexafluoroacetylacetonate)silver(I), Ag(hfac)-(1,5-COD), although many others have been used [99]. An ideal precursor should be $scCO_2$ soluble, be stable under high-pressure conditions, and degrade readily when required. The addition of fluorinated substituents has been shown to increase solubility in $scCO_2$ [55]. The addition of encapsulating ligands, such as multidentate chelates, completes the coordination sphere of the metal and essentially shields the metal from the $scCO_2$ [100]. The following impregnation procedure is representative of the method in general, but we will consider Ag(hfac)-(1,5-COD) as the example

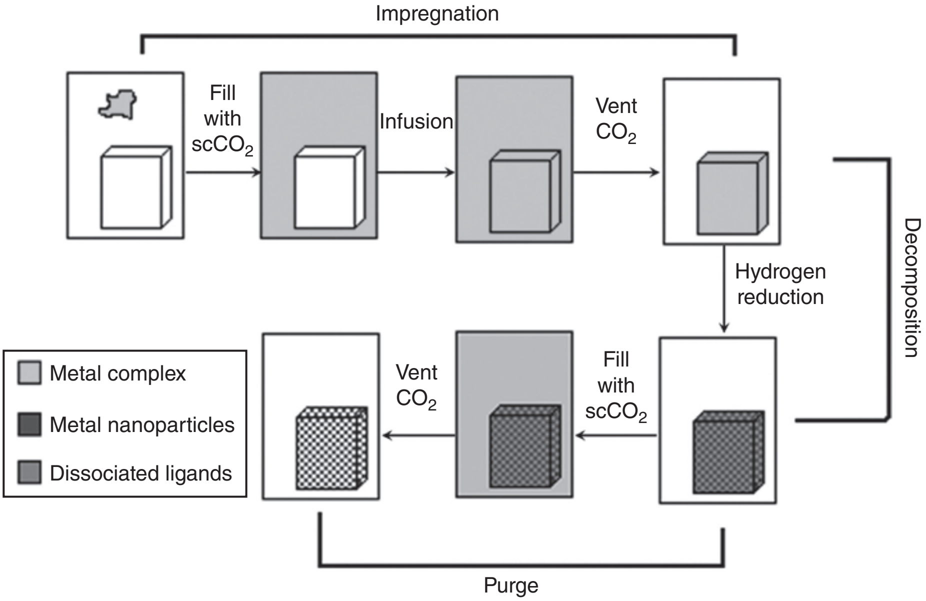

Figure 1.12. Schematic of a typical impregnation process as used by Howdle et al. consisting of three phases: impregnation, decomposition, and purging.

precursor. The impregnation process generally consists of three phases: impregnation, decomposition, and purge (Fig. 1.12). The first phase impregnates the precursor complex into the substrate. The precursor and substrate are placed in the autoclave, and the equipment is assembled before CO_2 is pumped in at a temperature just higher than the critical temperature of CO_2, for example, 40 °C. This ensures supercritical conditions while minimizing premature precursor decomposition. After leaving time for the infusion of the precursor into the substrate to occur (normally 24 hr), the autoclave is depressurized to vent the CO_2, leaving the precursor trapped in the substrate. Clearly, for this to happen effectively, it is essential that the precursor partitions into the polymer substrate. The second phase decomposes the precursor and leads to the formation of nanoparticles. In this step, the autoclave is filled with H_2 (typically at ~7 MPa) and heated to 80 °C to instigate the decomposition of the Ag precursor complex. This is thought to occur by a hydrogenolysis reaction resulting in Ag^0 and free dissociated ligands. The third phase is to repressurize the autoclave with $scCO_2$ at 40 °C, allowing the fluid to flow slowly through the autoclave for 24 hr to ensure complete extraction of the dissociated ligands. It is worth noting that this purging step is essential for processes in which by-products are undesirable, such as for antimicrobial materials that may be implanted in patients. However, for other materials, a negligible concentration of dissociated ligands might not be problematic, and this step can be omitted or shortened for expediency. This impregnation system has been used by Howdle et al. at the University of Nottingham to produce metal–polymer films for photonic [101, 102], catalytic [94],

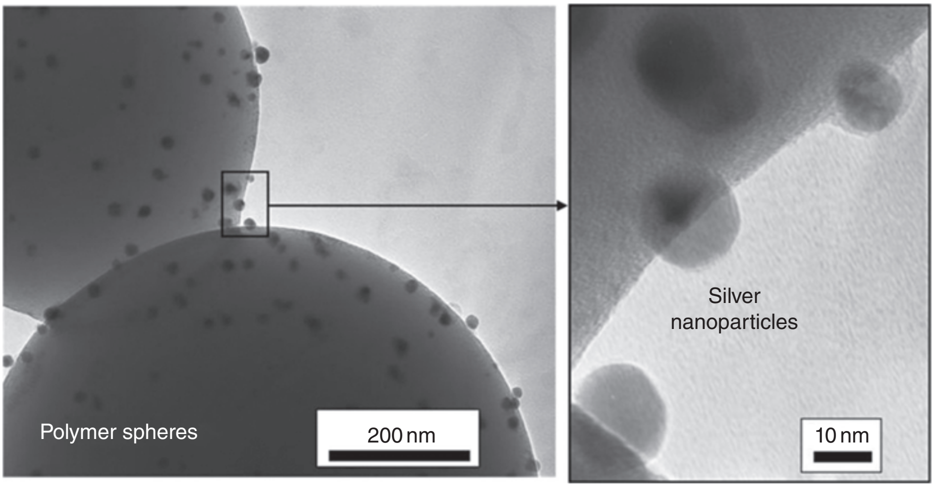

Figure 1.13. Bright-field TEM images detailing the surface location of the silver nanoparticles on PMMA microspheres following one-pot synthesis of silver–polymer nanocomposite in scCO2 in the presence of RAFT agent [103].

and medical applications [91, 92]. Following nanocomposite synthesis, there is always a need to characterize the particle morphology, size, distribution, and crystal structure of the metal phase inside the polymer matrix. This is particularly important when the properties of the metal nanoparticles are compared with their optical and biomedical performance. Among the characterization methods, transmission electron microscopy (TEM) is probably the most useful technique to directly probe the nanocomposites. Since the bulk polymer substrates tend to be too thick to transmit the electron beam, it is often necessary to microtome into transparent thin sections.

One striking alternative to the said process is a supercritical methodology that synthesizes not only the silver nanoparticles but also the polymer support in a simple process in $scCO_2$. Using reversible addition–fragmentation chain transfer (RAFT) polymerization agents, it is possible to produce silver nanoparticle-decorated polymer microspheres (Fig. 1.13) where the entire reaction takes place in a single step, in one pot, and in the absence of any conventional solvent [103]. In these reactions the polymer initiator is incorporated into the polymer surfactant, which is designed to also act as a stabilizing agent for the formation of metal nanoparticles, thus directing the nanoparticles onto the surface of the polymer spheres where they are ideally placed for many applications.

1.17 SILVER–POLYMER NANOCOMPOSITE FILMS FOR OPTICAL/PHOTONIC APPLICATIONS

Hasell et al. reported the clean impregnation of silver nanoparticles into a prefabricated polycarbonate strip in $scCO_2$, for application as an SERS device [101]. This method, even though producing nanoparticles inside the substrate *in situ*, did not cause any loss

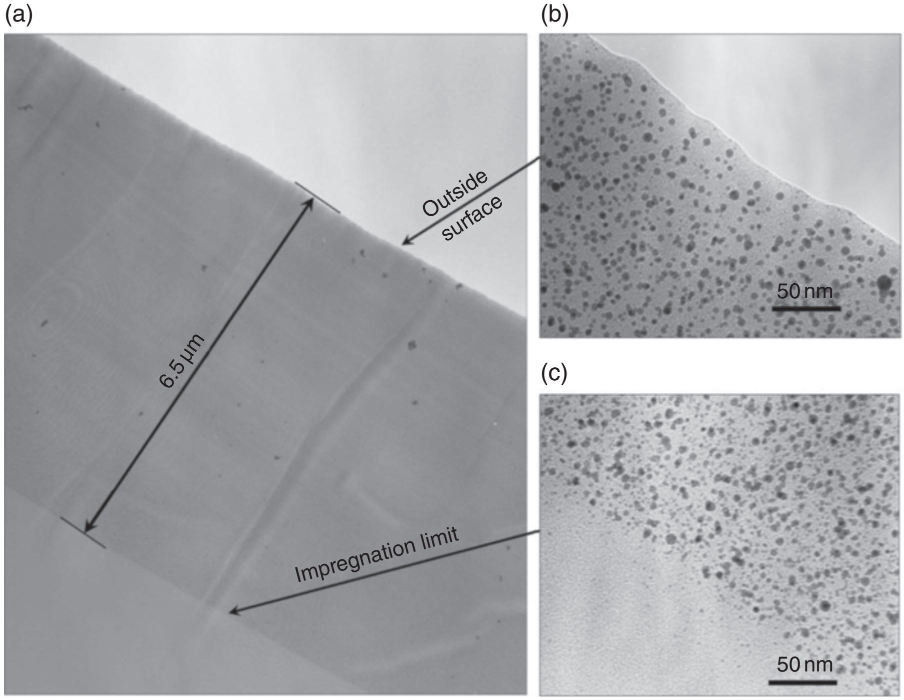

Figure 1.14. Bright-field TEM micrographs of a silver–polycarbonate nanocomposite sample prepared by cutting a 100 nm cross section of the material with an ultramicrotome fitted with a diamond blade. (**a**) The surface-located band of silver nanoparticles in the polycarbonate substrate. (**b**) A magnified section showing nanoparticles at the outside edge of the polymer. (**c**) A magnified section showing nanoparticles at the limit of furthest impregnation of the nanoparticles [101].

of transparency in the optical grade polymer. Transmission electron microscopy images of cross sections of the polymeric nanocomposite strips produced show clearly the silver nanoparticle distribution (Fig. 1.14). It is interesting to observe that there is a nanoparticle band of uniform thickness, of 6.5 µm, which runs along the outermost edge of the cross section of the polycarbonate substrate. There is a definite boundary of furthest impregnation. This was found to penetrate deeper, in a controllable manner, as a function of impregnation time. Discrete nanoparticles can be seen in the deposition band at the outermost surface of the polycarbonate, and they are roughly spherical in shape with an average diameter of 4.1 nm and a narrow size distribution. Such a silver–polycarbonate composite could allow the fabrication of optical and plasmonic devices that might exploit the mechanical robustness and flexibility of the polymers while providing protection of the particles from the surrounding environment (e.g., oxidation) to yield a high degree of temporal stability. The ability to precisely tune the impregnation depth of the nanoparticles on the micrometer scale gives this method an advantageous level of control for many potential applications.

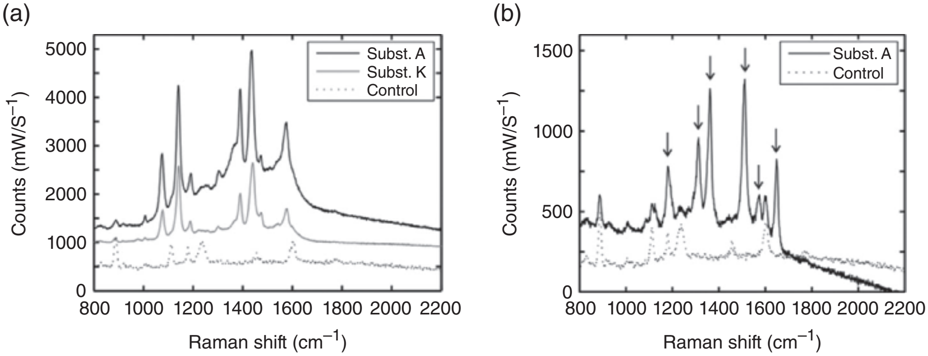

Figure 1.15. **(a)** Surface-enhanced Raman spectroscopy spectra of 4-ATP on the two metal–polycarbonate substrates (A and K) and **(b)** SERS spectrum of R6G taken on substrate A, where the arrows indicate the vibrational peaks of the dye. Both figures are plotted together with a control spectrum taken on undoped polycarbonate, and the spectra are offset for clarity.

The SERS activity of this nanocomposite was successfully demonstrated using both 4-aminothiophenol (4-ATP) and water-soluble Rhodamine 6G (R6G) as target molecules. These analytes were chosen because they have very distinct Raman features and form an ordered self-assembled monolayer on coinage-metal surfaces. The measured SERS spectra of the silver–polycarbonate film, following treatment with 4-ATP ethanol solution, are shown in Figure 1.15a. In comparison to a control sample of silver-free polycarbonate subject to identical treatment, the silver nanoparticle-loaded sample resulted in an enhancement factor greater than 10^7 of the Raman signal from the target molecule. Also, in the case of differently loaded samples, higher nanoparticle densities were found to lead to stronger SERS signals. A related investigation using R6G (Fig. 1.15b) suggests the overall SERS performance is also dependent on the bonding pattern of the target molecules to the silver.

Using the same silver–polycarbonate film substrate, Lagonigro et al. studied the time and spectrally resolved fluorescence [102]. Photoluminescence (PL) plays a crucial role in many aspects of biological and medical research with applications such as DNA sequencing [104], cell imaging [105], and sensing [106]. Large electric fields are generated by the plasmon modes of metal nanoparticles, and these can enhance photon–matter interaction to modify the excitation cross section [107] and the radiative decay rate. This phenomenon results in increased fluorescence intensities for molecules in close proximity to the metal [108]. Metal-enhanced fluorescence has led to the demonstration of optical probes with enhanced brightness, and these may play an important role in the next generation of photonic devices. This MEF activity further demonstrates the possible optical applications of silver nanostructures within polymer hosts. Metal-enhanced fluorescence measurement was conducted after a weak solution of coumarin 102, which served as a dye molecule, was spin coated onto the nanocomposite film substrate. The fluorescence spectra of coumarin 102, with time and spectral resolution,

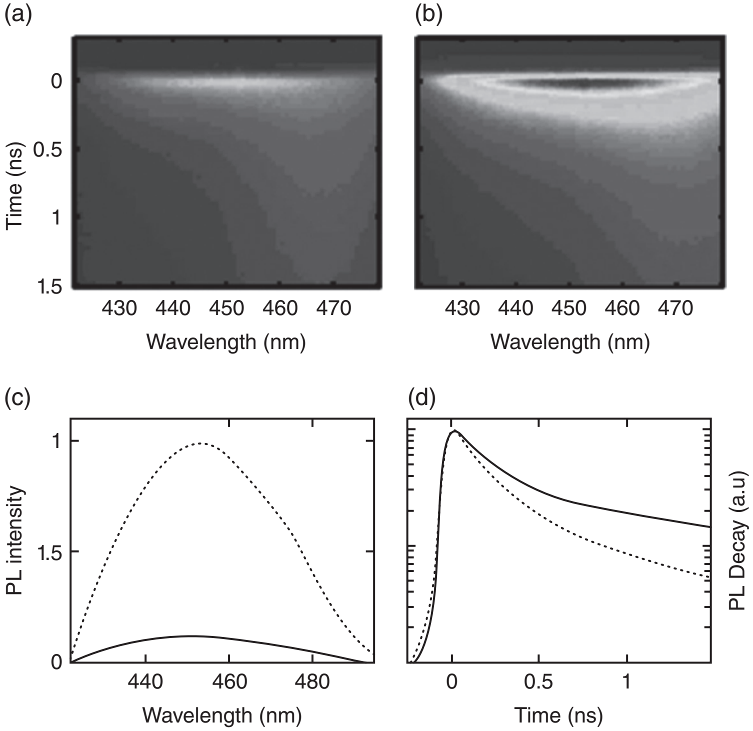

Figure 1.16. Time and spectrally resolved PL for coumarin on (**a**) silver-free polycarbonate and (**b**) silver–polycarbonate nanocomposite film. (**c**) Integrated PL spectra and (**d**) average PL decays on polycarbonate (solid) and silver-loaded polycarbonate (dotted). Reprinted with permission from Reference [102]. Copyright 2008, American Institute of Physics.

of both the silver-impregnated polycarbonate and silver-free polycarbonate are shown in Figure 1.16. The silver nanoparticles inside the polycarbonate give an enhancement of ~8.5 times the emission intensity, accompanied by a reduction in the photon lifetime. These preliminary investigations show how the excellent plasmonic properties of silver nanoparticles can also be utilized to yield large electric fields in the vicinity of fluorophores. In order for MEF to be conveniently used in routine procedures, the substrates need to be robust, stable, and, most importantly, biocompatible. Polycarbonate is known to have excellent biocompatibility, as well as optical and mechanical properties [30], and these composite structures offer a number of advantages over previously reported metal–polymer substrates fabricated via surface functionalization [109]. Owing to the versatility of this supercritical technique and its applicability to a range of prefabricated polymer films and devices and the abundance of suitable metal precursors, such substrates can be readily tailored for a wide range of applications in medicine and biology.

1.18 SILVER–POLYMER NANOCOMPOSITE FILMS FOR ANTIMICROBIAL APPLICATIONS

Due to the development of antibiotic resistance in many strains of infectious diseases, there is a need for alternative antibacterial agents. Metallic silver has been used throughout history for the treatment of wounds and burns. This antimicrobial property is related to the amount and rate of silver released as ions, in which state it can bind to proteins in the bacterial cell wall and nuclear membrane, leading to cell distortion and death. It is because of this effect that nanoparticlulate silver has been found to be so effective due to its large surface to volume ratio and crystallographic surface structure. Polymers are extensively used for medical and healthcare products because of their low toxicity and high biocompatibility, making them ideal hosts for biochemically active inorganic species. Polymeric substrates therefore offer a sustainable support to silver nanoparticles and allow such composites to be fabricated into devices. The bactericidal properties of silver nanoparticles have been shown to be size dependent; smaller nanoparticles, and especially those with diameters in the range of ~1–10 nm, have been shown to have the highest activity [110]. Supercritical processing is highly attractive as a route to produce clean silver–polymer nanocomposite materials for biomedical applications, leading Furno et al. to use $scCO_2$ for the impregnation of silver nanoparticles into a silicone support, which showed clear antimicrobial activity [93]. In order to determine the biomedical performance of the silver–polymer nanocomposites, the researchers investigated the release of silver ions, the adherence of silver to the substrate surface, and the killing of bacteria. The results of these tests suggest the nanocomposites have a clear persisting and diffusible activity to kill bacteria. Morley et al. later reported silver nanoparticle deposition into biodegradable ultrahigh-molecular-weight polyethylene (UHMWPE) using $scCO_2$ [92]. Ultrahigh-molecular-weight polyethylene is known as an extremely difficult substrate to process, which significantly demonstrates the ability of SCF processing to introduce metal nanoparticles into structures not accessible by conventional means. By *in situ* impregnation with $scCO_2$, nanocomposites with enhanced biocompatibility and antimicrobial activity were prepared. More recently, the same $scCO_2$ processing method was used to introduce silver nanoparticles into catheter tubing made of polydimethylsiloxane (PDMS) polymer. In this case an extended $scCO_2$ purge step was employed to ensure that all of the dissociated ligands were removed post processing [99]. The silver–PDMS nanocomposites produced were analyzed for their antimicrobial efficacy against a range of pathogens including the Gram-positive bacteria MRSA, the Gram-negative bacteria *E. coli*, and the yeast *C. albicans*. These silver–polymer composites showed significant activity towards both Gram-positive and Gram-negative adhered bacteria, eradicating 100% of adhered bacteria within the 72 hour time frame of the test. Furthermore, these tests demonstrated the viability of thorough CO_2 purging by showing there was no detectable residue of decomposed ligands left in the nanocomposites, as determined by gas chromatography with a detection limit of 7 ppm. This is particularly important since dissociated ligands from the precursor molecules used, such as the Ag(hfac)(1,5-COD) used in this instance, could have toxicological effects on surrounding tissues if implanted or indeed other unwanted effects in alternative medical or otherwise sensitive applications.

1.19 PALLADIUM–POLYMER NANOCOMPOSITE FILMS FOR CATALYSIS OR HYDROGEN UPTAKE APPLICATIONS

A research group at the University of Liverpool has demonstrated that the same simple impregnation strategy can also be used to introduce metal nanoparticles into the porous polymeric systems [111]. Microporous polymeric materials are receiving much current interest because of their potential applications in areas such as gas sorption, separation, and heterogeneous catalysis. Palladium nanoparticles were dispersed uniformly throughout a microporous poly(aryleneethynylene) material by the infusion of a CO_2-soluble Pd precursor, palladium(II) hexafluoroacetylacetonate. The resulting composite showed good thermal stability and has potential applications in gas storage and heterogeneous catalysis. The porosity of the polymeric support was maintained after inclusion of the metal, and the hydrogen uptake at room temperature was increased with respect to the unloaded porous support. Hydrogen storage by spillover has been suggested as a promising approach to enhancing the ambient-temperature hydrogen storage capacity of nanostructured materials. Conceptually, spillover involves the dissociation of hydrogen molecules on metal nanoparticles followed by subsequent hydrogen atom migration onto the nearby substrate by surface diffusion. Palladium can both chemisorb atomic hydrogen and also dissolve it to form bulk hydride phases and is capable of adsorbing hydrogen dissociatively and thereby act as a source of hydrogen atoms to migrate onto the substrate surface. Supported Pd nanoparticles are also relevant as catalysts for organic and industrial reactions. It is important for many of these applications that the nanoparticles should be small in size and well dispersed in a robust support of high surface area. It has been demonstrated that conjugated microporous polymer (CMP) systems are able to function as effective support and stabilization substrates for active metal nanoparticles, such as palladium [112]. The target substrate used for the $scCO_2$ deposition of Pd nanoparticles was based on a CMP [113] material. These CMP networks have a tunable micropore size distribution and surface area that is controlled by the length of the rigid organic linkers. Conjugated microporous polymers are relatively thermally robust and chemically stable. In this case, the impregnation of a conjugated poly(aryleneethynylene) polymer with palladium nanoparticles was achieved using the same general strategy described earlier and a relatively simple experimental setup (Fig. 1.17). The use of hydrogen for the reduction step was omitted as it was found that simple heating, to over 300 °C, could be more simply used to form nanoparticles as the polymer was stable to these high temperatures.

The results found for the impregnation step in this research provide an ideal example to discuss what is known as the partitioning effect. In order to introduce an SCF-soluble species into an insoluble substrate, the highest pressure (and therefore highest density and solubility) is very rarely found to be the optimal condition. The mass increase of the polymer after impregnation demonstrates the efficiency of the loading (Fig. 1.18). The optimum pressure was found to be ~8 MPa, just above the critical pressure of CO_2 (7.38 MPa). This can be explained by two competing factors: solubility and solid–fluid partitioning. At lower pressures, the Pd complex is not soluble enough to be effectively transported into the polymer, whereas at higher pressures, the solubility increases to the point that the Pd complex preferentially partitions into the CO_2 outside of the polymer.

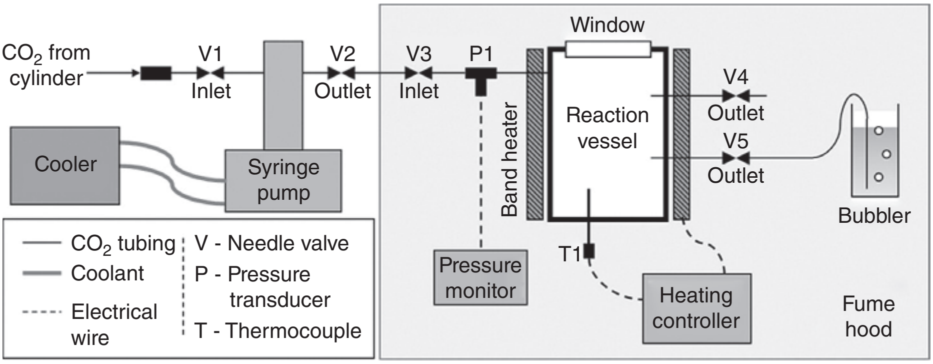

Figure 1.17. Schematic representation of the equipment used for the supercritical impregnation. The reaction vessel consists of a 10 cm³ volume stainless steel autoclave fitted with a sapphire view window. Pressure is controlled by the syringe pump, heating by an external heater with internal thermocouple, and venting speed by using an outlet bubbler [111].

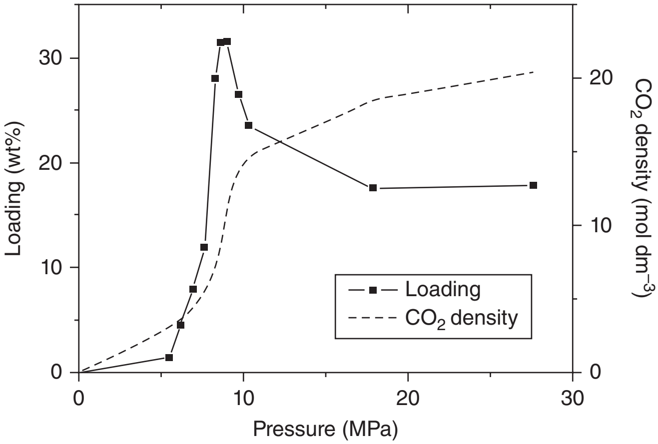

Figure 1.18. Loading of Pd complex as a function of CO_2 pressure at 40 °C [111].

Investigation of the products by scanning and TEM (Fig. 1.19) revealed larger nanoparticles on the surface of the polymer with smaller nanoparticles inside the polymer network. The ~5–10 nm surface-bound nanoparticles were ascribed to Pd complex that was deposited on the surface during depressurization. These particles were able to grow more freely and hence agglomerate, whereas the growth of particles formed inside the microporous network was restricted by the pore dimensions. The nanoparticles inside the network were found to be limited to ~1–3 nm in diameter, in close agreement with the average diameter of the pores of the polymer. The large number of smaller nanoparticles as well as their dispersed nature throughout the pores of the substrate would be difficult to achieve with conventional impregnation techniques, such as solvent infusion or CVD.

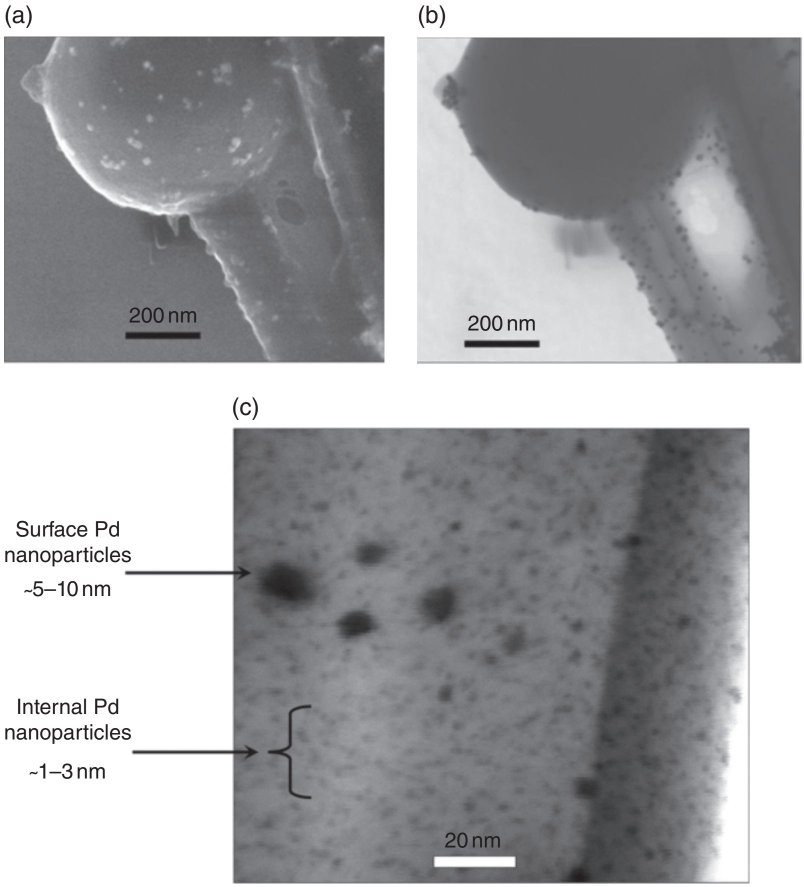

Figure 1.19. Electron microscopy of a Pd-loaded CMP sample. (**a**) Scanning mode image (left) and (**b**) transmission mode (right) of the same area of microporous polymer. At this magnification, only larger nanoparticles located on the surface are visible. (**c**) Under higher-magnification transmission mode, a bimodal nanoparticle size distribution is observed where the smaller, internally located nanoparticles can be observed [111].

Smaller nanoparticles and extensive dispersion are in principle desirable for increased hydrogen uptake. Gas sorption measurements of these polymers indicated that porosity was maintained after impregnation of Pd nanoparticles and that hydrogen uptake, at room temperature and low pressure, was significantly enhanced by the addition of the nanoparticles (Fig. 1.20). This research showed that in addition to conventional polymers, $scCO_2$ is also able to provide a simple and effective processing route to generate metal nanoparticles *in situ* within prefabricated CMPs. The nanoparticles are well dispersed throughout the material and show excellent size control within the pore matrix. Such polymer–metal composite materials may have future advantages over materials such as carbon because they can couple greater synthetic versatility with

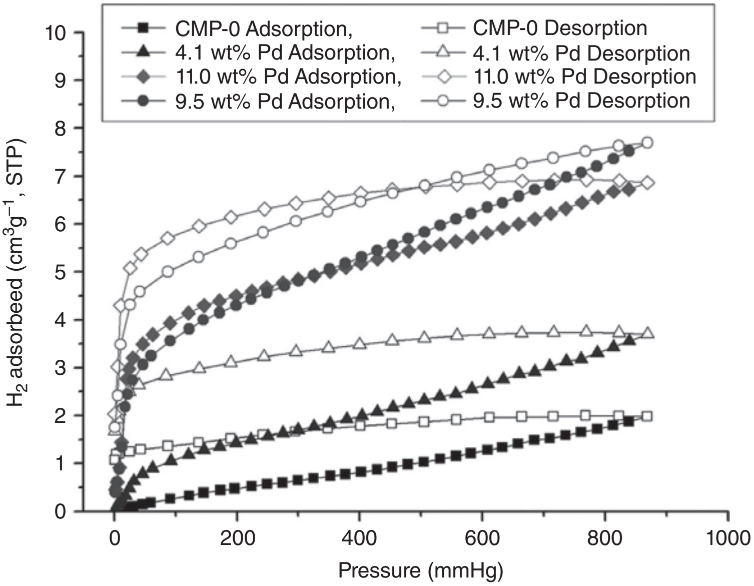

Figure 1.20. Low-pressure H_2 isotherms at 20 °C for a series of microporous polymer samples. The hydrogen uptake is significantly increased by the inclusion of Pd nanoparticles.

adequate thermal and chemical robustness. Such systems may have potential as substrates for hydrogen spillover—for example, in catalytic processes—but the amounts of H_2 adsorbed at ambient temperature are still below the levels that are interesting for practical gas storage applications.

1.20 CONCLUSIONS

This chapter has outlined the importance of the emergent field of nanocomposite functional materials and has shown that the development of new routes to metal–polymer nanocomposites is a relevant and necessary area of study. An introduction and overview into the fields of nanoparticles, polymers, and SCFs has been provided, with the intention of giving readers with no previous knowledge of these fields sufficient background knowledge.

The work reported in this chapter demonstrates the possibility of using $scCO_2$ techniques for the formation of optical quality polymer–metal nanocomposite material. It has been shown that $scCO_2$ is a viable technique to produce uniform and transparent plasmonic nanocomposites. The polymeric substrate (polycarbonate) is regularly used to construct optical devices such as lenses and windows. As the nanoparticles are introduced *in situ* and post fabrication of the material, without loss of transparency, it is easy to see the possible benefits of using such a system to introduce metal particles into devices after they have been processed into the final form. This neatly avoids any aggregation or degradation of the uniform nanoparticle distribution that would occur during the fabrication of polymer feedstock into a desired architecture. The impregnation process shows good potential for control of both depth and size/concentration of the nanoparticles by modification of time and pressure variables. The products have been demonstrated as excellent SERS and MEF enhancement materials, which could find application in the next generation of plasmonic devices and sensors and in particular biological or in vivo monitoring. These substrates offer a number of significant benefits in that they are cheap, flexible, mechanically robust, and temporally stable so that they can be stored for long lengths of time, easily handled and discarded after use to avoid cross contamination. There are a wide range of optical and biomedical potential applications, and a key conclusion is that $scCO_2$ provides a very flexible and clean route to novel materials and properties.

It has been illustrated that as well as impregnating preformed solid polymers with metal nanoparticles, it is also possible to directly synthesis the polymer itself at the same time as the metal nanoparticles, all taking place in carbon dioxide. This was achieved by the use of an appropriately designed RAFT/stabilizing agent that allows simple and effective synthesis of polymer microspheres decorated with silver nanoparticles. The surface location of the nanoparticles gives the polymer powder excellent potential for catalytic, antibacterial, and biosensing applications. This synthetic route has the additional advantages of being a single step, one-pot reaction that does not require conventional solvents at any stage during the process. Furthermore, the versatility of this technique suggests its applicability for a wide range of polymer nanoparticle composite materials.

Supercritical CO_2 has also been shown to provide a simple and effective processing route to generate metal nanoparticle-loaded CMPs. The nanoparticles are again well dispersed throughout the material and show excellent size control within the pore matrix.

There are certainly limitations to the use of $scCO_2$, for example, in the solubility of reagents and the necessity of using high pressures, and it certainly does not provide a universal solution to making nanocomposites. However, there are also clear benefits and specific examples where materials can be fabricated using $scCO_2$ that simply could not be accessed using conventional technologies. Whatever routes are chosen, it is clear that by improving the quality of the nanocomposites and understanding the mechanism of their optical and biomedical activities, useful devices for practical applications will result.

REFERENCES

[1] L. Nicolais and G. Carotenuto, *Metal-Polymer Nanocomposites*, Wiley, Hoboken, 2005.

[2] E. Roduner, *Chemical Society Reviews*, 2006, **35**, 583–592.

[3] C. N. R. Rao, P. J. Thomas and G. U. Kulkarni, *Nanocrystals: Synthesis, Properties and Applications*, Springer, Berlin-Heidelberg-New York, 2007.

[4] F. Raimondi, G. G. Scherer, R. Kotz and A. Wokaun, *Angewandte Chemie-International Edition*, 2005, **44**, 2190–2209.

[5] C. R. Henry, *Surface Science Reports*, 1998, **31**, 231–325.

[6] A. Haruta, *Chemical Record*, 2003, **3**, 75–87.

[7] M. Haruta, *Cattech*, 2002, **6**, 102–115.

[8] M. Haruta and M. Date, *Applied Catalysis a-General*, 2001, **222**, 427–437.

[9] M. C. Daniel and D. Astruc, *Chemical Reviews*, 2004, **104**, 293–346.

[10] F. Boccuzzi, A. Chiorino, M. Manzoli, P. Lu, T. Akita, S. Ichikawa and M. Haruta, *Journal of Catalysis*, 2001, **202**, 256–267.

[11] M. Mavrikakis, P. Stoltze and J. K. Norskov, *Catalysis Letters*, 2000, **64**, 101–106.

[12] P. N. Prasad, *Current Opinion In Solid State & Materials Science*, 2004, **8**, 11–19.

[13] D. J. Norris and M. G. Bawendi, *Physical Review B*, 1996, **53**, 16338–16346.

[14] G. Schmid, *Nanoparticles: From Theory to Applications*, Wiley, New York, 2004.

[15] C. F. Bohren and D. R. Huffman, *Absorption and Scattering of Light by Small Particles*, Wiley, New York, 1983.

[16] P. N. Prasad, *Nanophotonics*, Wiley, Hoboken, New Jersey, 2004.

[17] K. L. Kelly, E. Coronado, L. L. Zhao and G. C. Schatz, *Journal of Physical Chemistry B*, 2003, **107**, 668–677.

[18] N. K. Grady, N. J. Halas and P. Nordlander, *Chemical Physics Letters*, 2004, **399**, 167–171.

[19] S. Link and M. A. El-Sayed, *Journal of Physical Chemistry B*, 1999, **103**, 8410–8426.

[20] D. D. Evanoff and G. Chumanov, *Chemphyschem*, 2005, **6**, 1221–1231.

[21] Z. X. Liu, H. H. Wang, H. Li and X. M. Wang, *Applied Physics Letters*, 1998, **72**, 1823–1825.

[22] S. Shi, W. Ji, S. H. Tang, J. P. Lang and X. Q. Xin, *Journal of American Chemical Society*, 1994, **116**, 3615–3616.

[23] Y. P. Sun, J. E. Riggs, H. W. Rollins and R. Guduru, *Journal of Physical Chemistry B*, 1999, **103**, 77–82.

[24] L. Francois, M. Mostafavi, J. Belloni, J. F. Delouis, J. Delaire and P. Feneyrou, *Journal of Physical Chemistry B*, 2000, **104**, 6133–6137.

[25] R. B. Martin, M. J. Meziani, P. Pathak, J. E. Riggs, D. E. Cook, S. Perera and Y. P. Sun, *Optical Materials*, 2007, **29**, 788–793.

[26] V. Liberman, M. Rothschild, O. M. Bakr and F. Stellacci, *Journal of Optics*, 2010, **12**.

[27] S. Porel, N. Venkatrarn, D. N. Rao and T. P. Radhakrishnan, *Journal of Applied Physics*, 2007, **102**.

[28] E. Smith and G. Dent, *Modern Raman Spectroscopy - A Practical Approach*, Wiley, Chichester, 2005.

[29] K. Kneipp, Y. Wang, H. Kneipp, L. T. Perelman, I. Itzkan, R. Dasari and M. S. Feld, *Physical Review Letters*, 1997, **78**, 1667–1670.

[30] K. Aslan, P. Holley and C. D. Geddes, *Journal Of Materials Chemistry*, 2006, **16**, 2846–2852.

[31] K. Aslan, I. Gryczynski, J. Malicka, E. Matveeva, J. R. Lakowicz and C. D. Geddes, *Current Opinion in Biotechnology*, 2005, **16**, 55–62.

[32] J. P. Abid, A. W. Wark, P. F. Brevet and H. H. Girault, *Chemical Communications*, 2002, 792–793.

[33] H. H. Huang, X. P. Ni, G. L. Loy, C. H. Chew, K. L. Tan, F. C. Loh, J. F. Deng and G. Q. Xu, *Langmuir*, 1996, **12**, 909–912.

[34] S. A. Dong and S. P. Zhou, *Materials Science and Engineering B-Solid State Materials for Advanced Technology*, 2007, **140**, 153–159.

[35] H. Hirai, Y. Nakao and N. Toshima, *Journal of Macromolecular Science-Chemistry*, 1979, **A13**, 727–750.

[36] M. Brust, M. Walker, D. Bethell, D. J. Schiffrin and R. Whyman, *Journal of the Chemical Society-Chemical Communications*, 1994, 801–802.

[37] J. A. Creighton, C. G. Blatchford and M. G. Albrecht, *Journal Of The Chemical Society-Faraday Transactions Ii*, 1979, **75**, 790–798.

[38] P. C. Lee and D. Meisel, *Journal Of Physical Chemistry*, 1982, **86**, 3391–3395.

[39] H. Bonnemann and R. M. Richards, *European Journal Of Inorganic Chemistry*, 2001, 2455–2480.

[40] M. V. Volpe, A. Longo, L. Pasquini, V. Casuscelli and G. Carotenuto, *Journal Of Materials Science Letters*, 2003, **22**, 1697–1699.

[41] G. Carotenuto and L. Nicolais, *Journal of Materials Chemistry*, 2003, **13**, 1038–1041.

[42] E. Hutter and J. H. Fendler, *Advanced Materials*, 2004, **16**, 1685–1706.

[43] G. Carotenuto, B. Martorana, P. B. Perlo and L. Nicolais, *Journal of Material Chemistry*, 2003, **13**, 2927–2930.

[44] S. Matsuda and S. Ando, *Japanese Journal of Applied Physics Part 1-Regular Papers Short Notes & Review Papers*, 2005, **44**, 187–192.

[45] S. Porel, S. Singh, S. S. Harsha, D. N. Rao and T. P. Radhakrishnan, *Chemical Matters*, 2005, **17**, 9–12.

[46] S. Matsuda, S. Ando and T. Sawada, *Electron. Lett.*, 2001, **37**, 706–707.

[47] A. V. Gaikwad and T. K. Rout, *Journal of Materials Chemistry*, 2011, **21**, 1234–1239.

[48] S. Koizumi, S. Matsuda and S. Ando, *Journal of Photopolymer Science and Technology*, 2002, **15**, 231–236.

[49] A. L. Stepanov, S. N. Abdullin, V. Y. Petukhov, Y. N. Osin, R. I. Khaibullin and I. B. Khaibullin, *Philosophical Magazine B*, 2000, **80**, 23–28.

[50] A. L. Stepanov, S. N. Abdullin and I. B. Khaibullin, *Journal of Non-Crystalline Solids*, 1998, **223**, 250–253.

[51] M. Okumura, S. Nakamura, S. Tsubota, T. Nakamura, M. Azuma and M. Haruta, *Catalysis Letters*, 1998, **51**, 53–58.

[52] T. Clifford, *Fundamentals of Supercritical Fluid*. OUP, Oxford, 1999.

[53] T. Andrews, *Philosophical Magazine*, 1870, 150–153.

[54] J. B. Hannay and J. Hogarth, *Proceedings of Royal Society B London*, 1879, **29**, 324–326.

[55] J. A. Darr and M. Poliakoff, *Chemical Reviews*, 1999, **99**, 495–541.

[56] A. I. Cooper, *Journal of Material Chemistry*, 2000, **10**, 207–234.

[57] F. Furno, P. Licence, S. M. Howdle and M. Poliakoff, *Actualite Chimique*, 2003, 62–66.

[58] J. R. Hyde, P. Licence, D. Carter and M. Poliakoff, *Applied Catalysis a-General*, 2001, **222**, 119–131.

[59] E. J. Beckman, *Journal of Supercritical Fluids*, 2004, **28**, 121–191.

[60] C. F. Kirby and M. A. McHugh, *Chemical Reviews*, 1999, **99**, 565–602.

[61] D. L. Tomasko, H. B. Li, D. H. Liu, X. M. Han, M. J. Wingert, L. J. Lee and K. W. Koelling, *Industrial and Engineering Chemistry Research*, 2003, **42**, 6431–6456.

[62] J. L. Kendall, D. A. Canelas, J. L. Young and J. DeSimone, *Chemical Reviews*, 1999, **99**, 543–563.

[63] W. Wang, A. Naylor and S. M. Howdle, *Macromolecules*, 2003, **36**, 5424–5427.

[64] C. D. Wood and A. I. Cooper, *Macromolecules*, 2001, **34**, 5–8.

[65] J. M. Desimone, Z. Guan and C. S. Elsbernd, *Science*, 1992, **257**, 945–947.

[66] J. M. Desimone, E. E. Maury, Y. Z. Menceloglu, J. B. McClain, T. J. Romack and J. R. Combes, *Science*, 1994, **265**, 356–359.

[67] P. Christian, M. R. Giles, R. M. T. Griffiths, D. J. Irvine, R. C. Major and S. M. Howdle, *Macromolecules*, 2000, **33**, 9222–9227.

[68] P. Christian, S. M. Howdle and D. J. Irvine, *Macromolecules*, 2000, **33**, 237–239.

[69] H. M. Woods, M. Silva, C. Nouvel, K. M. Shakesheff and S. M. Howdle, *Journal of Materials Chemistry*, 2004, **14**, 1663–1678.

[70] K. J. Thurecht, A. M. Gregory, S. Villarroya, J. X. Zhou, A. Heise and S. M. Howdle, *Chemical Communications*, 2006, 4383–4385.

[71] S. Villarroya, K. J. Thurecht, A. Heise and S. M. Howdle, *Chemical Communications*, 2007, 3805–3813.

[72] S. Villarroya, K. J. Thurecht and S. M. Howdle, *Green Chemistry*, 2008, **10**, 863–867.

[73] J. X. Zhou, S. Villarroya, W. X. Wang, M. F. Wyatt, C. J. Duxbury, K. J. Thurecht and S. M. Howdle, *Macromolecules*, 2007, **40**, 2276–2276.

[74] I. Kikic and F. Vecchione, *Current Opinion in Solid State & Materials Science*, 2003, **7**, 399–405.

[75] Y. Zhang and C. Erkey, *Journal of Supercritical Fluids*, 2006, **38**, 252–267.

[76] J. J. Watkins and T. J. McCarthy, *Chemistry of Materials*, 1995, **7**, 1991.

[77] R. Kumar, S. Roy, M. Rashidi and R. J. Puddephatt, *Polyhedron*, 1989, **8**, 551–553.

[78] Y. F. Zong and J. J. Watkins, *Chemistry of Materials*, 2005, **17**, 560–565.

[79] A. Cabanas, D. P. Long and J. J. Watkins, *Chemistry of Materials*, 2004, **16**, 2028–2033.

[80] E. T. Hunde and J. J. Watkins, *Chemistry of Materials*, 2004, **16**, 498–503.

[81] A. Cabanas, X. Y. Shan and J. J. Watkins, *Chemistry of Materials*, 2003, **15**, 2910–2916.

[82] A. Cabanas, J. M. Blackburn and J. J. Watkins, *Microelectronic Engineering*, 2002, **64**, 53–61.

[83] J. M. Blackburn, D. P. Long, A. Cabanas and J. J. Watkins, *Science*, 2001, **294**, 141–145.

[84] X. R. Ye, J. B. Talbot, S. H. Jin, Y. H. Lin and C. M. Wai, *Abstracts of Papers of the American Chemical Society*, 2005, **229**, U926–U926.

[85] X. R. Ye, Y. H. Lin, C. M. Wai, J. B. Talbot and S. H. Jin, *Journal of Nanoscience and Nanotechnology*, 2005, **5**, 964–969.

[86] X. R. Ye, H. F. Zhang, Y. H. Lin, L. S. Wang and C. M. Wai, *Journal of Nanoscience and Nanotechnology*, 2004, **4**, 82–85.

[87] X. R. Ye, Y. H. Lin, C. M. Wang, M. H. Engelhard, Y. Wang and C. M. Wai, *Journal of Materials Chemistry*, 2004, **14**, 908–913.

[88] C. D. Saquing, D. Kang, M. Aindow and C. Erkey, *Microporous and Mesoporous Materials*, 2005, **80**, 11–23.

[89] Y. Zhang, D. F. Kang, C. Saquing, M. Aindow and C. Erkey, *Industrial & Engineering Chemistry Research*, 2005, **44**, 4161–4164.

[90] K. S. Morley, P. Licence, P. C. Marr, J. R. Hyde, P. D. Brown, R. Mokaya, Y. D. Xia and S. M. Howdle, *Journal Of Materials Chemistry*, 2004, **14**, 1212–1217.

[91] K. S. Morley, P. C. Marr, P. B. Webb, A. R. Berry, F. J. Allison, G. Moldovan, P. D. Brown and S. M. Howdle, *Journal Of Materials Chemistry*, 2002, **12**, 1898–1905.

[92] K. S. Morley, P. B. Webb, N. V. Tokareva, A. P. Krasnov, V. K. Popov, J. Zhang, C. J. Roberts and S. M. Howdle, *European Polymer Journal*, 2007, **43**, 307–314.

[93] F. Furno, K. S. Morley, B. Wong, B. L. Sharp, P. L. Arnold, S. M. Howdle, R. Bayston, P. D. Brown, P. D. Winship and H. J. Reid, *Journal of Antimicrobial Chemotherapy*, 2004, **54**, 1019–1024.

[94] B. Wong, S. Yoda and S. M. Howdle, *Journal of Supercritical Fluids*, 2007, **42**, 282–287.

[95] R. K. Boggess, L. T. Taylor, D. M. Stoakley and A. K. StClair, *Journal of Applied Polymer Science*, 1997, **64**, 1309–1317.

[96] S. Yoda, A. Hasegawa, H. Suda, Y. Uchimaru, K. Haraya, T. Tsuji and K. Otake, *Chemistry Of Materials*, 2004, **16**, 2363–2368.

[97] H. Suda, S. Yoda, A. Hasegawa, T. Tsuji, K. Otake and K. Haraya, *Desalination*, 2006, **193**, 211–214.

[98] S. Yoda, Y. Takebayashi, T. Sugeta and K. Otake, *Journal Of Non-Crystalline Solids*, 2004, **350**, 320–325.

[99] J. X. Yang, T. Hasell, D. C. Smith and S. M. Howdle, *Journal of Materials Chemistry*, 2009, **19**, 8560–8570.

[100] K. Morley, *The clean preparation of nanocomposite materials: a supercritical route*, PhD Thesis, University of Nottingham, 2003.

[101] T. Hasell, L. Lagonigro, A. C. Peacock, S. Yoda, P. D. Brown, P. J. A. Sazio and S. M. Howdle, *Advanced Functional Materials*, 2008, **18**, 1265–1271.

[102] L. Lagonigro, A. C. Peacock, S. Rohrmoser, T. Hasell, S. M. Howdle, P. J. A. Sazio and P. G. Lagoudakis, *Applied Physics Letters*, 2008, **93**.

[103] T. Hasell, K. J. Thurecht, R. D. W. Jones, P. D. Brown and S. M. Howdle, *Chemical Communications*, 2007, 3933–3935.

[104] L. M. Smith, J. Z. Sanders, R. J. Kaiser, P. Hughes, C. Dodd, C. R. Connell, C. Heiner, S. B. H. Kent and L. E. Hood, *Nature*, 1986, **321**, 674–679.

[105] D. J. Stephens and V. J. Allan, *Science*, 2003, **300**, 82–86.

[106] P. K. Jain, X. Huang, I. H. El-Sayed and M. A. El-Sayad, *Plasmonics*, 2007, **2**, 107–118.

[107] J. S. Biteen, D. Pacifici, N. S. Lewis and H. A. Atwater, *Nano Letters*, 2005, **5**, 1768–1773.

[108] J. R. Lakowicz, *Analytical Biochemistry*, 2005, **337**, 171–194.

[109] K. Aslan, Z. Leonenko, J. R. Lakowicz and C. D. Geddes, *Journal of Fluorescence*, 2005, **15**, 643–654.

[110] M. Rai, A. Yadav and A. Gade, *Biotechnology Advances*, 2009, **27**, 76–83.

[111] T. Hasell, C. D. Wood, R. Clowes, J. T. A. Jones, Y. Z. Khimyak, D. J. Adams and A. I. Cooper, *Chem. Mat.*, 2010, **22**, 557–564.

[112] J. Schmidt, J. Weber, J. D. Epping, M. Antonietti and A. Thomas, *Advanced Materials*, 2009, **21**, 702.

[113] J. X. Jiang, F. Su, A. Trewin, C. D. Wood, N. L. Campbell, H. Niu, C. Dickinson, A. Y. Ganin, M. J. Rosseinsky, Y. Z. Khimyak and A. I. Cooper, *Angewandte Chemie-International Edition*, 2008, **47**, 1167–1167.